LAPPEENRANTA
UNIVERSITY OF TECHNOLOGY

Antti Puisto

THE INITIAL OXIDATION OF TRANSITION METAL SURFACES

Thesis for the degree of Doctor of Science (Technology) to be presented with due permission for public examination and criticism in the Auditorium 1382 at Lappeenranta University of Technology, Lappeenranta, Finland on the 18th of April, 2008, at noon.

Acta Universitatis
Lappeenrantaensis
305

Supervisor Professor Matti Alatalo
Department of Electrical Engineering
Lappeenranta University of Technology
Lappeenranta, Finland

Reviewers Professor Hannu Häkkinen
Department of Physics
Nanoscience center
University of Jyväskylä
Jyväskylä, Finland

Dr. Christopher Latham
Department of Chemistry
University of Sussex
Falmer
Brighton
BN1 9QJ
United Kingdom

Opponent Professor Mario Rocca
Department of Physics
University of Genova
Genova, Italy

ISBN 978-952-214-557-4
ISBN 978-952-214-558-1 (PDF)
ISSN 1456-4491

Lappeenrannan teknillinen yliopisto
Digipaino

Abstract

Antti Puisto
The initial oxidation of transition metal surfaces
Lappeenranta 2008
59 p.
Acta Universitatis Lappeenrantaensis 305
Diss. Lappeenranta University of Technology
ISBN 978-952-214-557-4, ISBN 978-952-214-558-1 (PDF), ISSN 1456-4491

Due to their numerous novel technological applications ranging from the example of exhaust catalysts in the automotive industry to the catalytic production of hydrogen, surface reactions on transition metal substrates have become to be one of the most essential subjects within the surface science community. Although numerous applications exist, there are many details in the different processes that, after many decades of research, remain unknown.

There are perhaps as many applications for the corrosion resistant materials such as stainless steels. A thorough knowledge of the details of the simplest reactions occuring on the surfaces, such as oxidation, play a key role in the design of better catalysts, or corrosion resistant materials in the future.

This thesis examines the oxidation of metal surfaces from a computational point of view mostly concentrating on copper as a model material. Oxidation is studied from the initial oxidation to the oxygen precovered surface. Important parameters for the initial sticking and dissociation are obtained.

The saturation layer is thoroughly studied and the calculated results are compared with available experimental results. On the saturated surface, some open questions still remain. The present calculations demonstrate, that the saturated part of the surface is excluded from being chemically reactive towards the oxygen molecules. The results suggest, that the reason for the chemical activity of the saturated surface is due to a strain effect occuring between the saturated areas of the surface.

Keywords: *surface physics, adsorption, oxidation, metal surfaces*
UDC 539.233 : 542.943 -034.3

Preface

This thesis was prepared at Lappeenranta University of Technology, Department of Electrical Engineering, Laboratory of Electronics Materials Science under the guidance of Professor Matti Alatalo during the years 2004-2008.

I wish to thank Professor Alatalo for giving me the opportunity to work at the University, and for his encouracement and enthusiastic attitude towards my work. I also thank my colleagues at the 'play room', particularly Matti, Sami, Nelli, and Heikki who all have one way or another participated the studies included in this thesis. Many thanks also to Jani Peusaari for all the help in administrating our local computer resources; your work has been very important to the production of this thesis.

Thank you for all the people in Laboratory of Physics at HUT, Surface Science Laboratory at TUT, and Chemistry Department at University of Oulu, with whom I have had the privilege to collaborate over the years. Special thanks goes to Sampsa Jaatinen for the particularly inspirational discussions during all those numerous scientific meetings.

I acknowledge the reviewers Professor Hannu Häkkinen and Dr. Christopher Latham for their valuable comments, and especially Dr. Latham, for the language related corrections. I would have really struggled without you. I am also grateful for Professor Mario Rocca, for his efforts as the opponent.

The work is partly supported by the Finnish Cultural Foundation. The generous computer resources by CSC the Finnish IT centre are also gratefully acknowledged. The personnel in the LUT computing centre have also certainly given their best during the years.

Finally, I thank my family for supporting me all the way through.

Lappeenranta, March 2008

Antti Puisto

List of Publications

This thesis consists of an overview and the following publications

I A. Puisto, H. Pitkänen, M. Alatalo, S. Jaatinen, P. Salo, A. S. Foster, T. Kangas, K. Laasonen, Adsorption of atomic and molecular oxygen on Cu(100), Catalysis Today 100, 403 (2005).

II M. Hirsimäki, M. Ahonen, A. Puisto, S. Auvinen, M. Valden, and M. Alatalo, On the reactivity of vacancies, steps and adatoms on Cu(100) towards O_2 dissociation, submitted to Chem. Phys. Lett.

III M. Alatalo, A. Puisto, H. Pitkänen, A. S. Foster, and K. Laasonen, Adsorption dynamics of O_2 on Cu(100), Surf. Sci. 600, 1574 (2006).

IV S. Jaatinen, J. Blomqvist, P. Salo, A. Puisto, M. Alatalo, M. Hirsimäki, M. Ahonen, and M. Valden, Adsorption and diffusion dynamics of atomic and molecular oxygen on reconstructed Cu(100), Phys. Rev B 75, 075402 (2007).

V M. Lahti, N. Nivalainen, A. Puisto, M. Alatalo, O_2 dissociation on Pd(211) and Cu(211) surfaces, Surf. Sci. 601, 3774 (2007).

Authors contribution. The author has written publications III-V and actively participated in writing publications I and II. Most of the simulations in Publications I, II and III and the simulations involving O_2 in publication IV were performed by the author. The author has played very active role in the interpretation of the calculated results in every Publication. In publication V the author also contributed to the calculations by optimizing the basis sets for each material.

Other relevant papers by the author, related to the present thesis.

VI T. Kangas, K. Laasonen, A. Puisto, H. Pitkänen, M. Alatalo, On-surface and sub-surface oxygen on ideal and reconstructed Cu(100), Surf. Sci. 584, 62 (2005).

VII T. Kangas, N. Nivalainen, H. Pitkänen, A. Puisto, M. Alatalo, and K. Laasonen, Oxygen induced segregation of copper to Ag/Cu(100) surface, Surf. Sci. 600, 4103 (2006).

VIII The role of preadsorbed sulphur and oxygen in O_2 dissociation on Pd(100), M. Lahti, A. Puisto, M. Alatalo, T. S. Rahman, Submitted to Surf. Sci.

Abbreviations

A	Prefactor
a	Acceleration
BO	Born-Oppenheimer (approximation)
CA	Ceperly-Alder (parametrization for LDA)
DFT	Density Functional Theory
E_{ads}	Adsorption energy
E_b	Barrier height
E_{dis}	Dissociation energy
E_{init}	Initial state energy
$E_{\text{s}_{\text{max}}}$	Maximum bond stretching energy
E_{slab}	Surface slab energy
E_{total}	Total energy of the slab and the adsorbate
E_{TS}	Transition state energy
E_{xc}	Exchange and correlation potential
F	Force
f_{max}	Maximum vibrational frequency
f_s	Sampling frequency
GGA	Generalized Gradient Approximation
H	Hamiltonian
$\hbar$	Dirac's constant
$\hat{H}$	Hamiltonian in operator notation
k	Frequency factor
LDA	Local Density Approximation
LSDA	Local Spin Density Approximation

m	Mass
MBSS	Molecular Beam Surface Scattering
MD	Molecular Dynamics
$\hat{n}(\vec{r})$	Fermion density operator
NAO	Numerical Atomic Orbitals
PAW	Projector Augmented Wave
PBE	Perdew-Burke-Ernzerhoff (GGA type)
PES	Potential Energy Surface
PW91	Perdew-Wang 91 (GGA type)
R_i	Coordinate of an atomic nucleus
S1, S2, S6	Surface phonon modes
STM	Scanning Tunneling Microscopy
SIESTA	Spanish Initiative for Electronic Simulations with Thousands of Atoms (program package)
$\hat{T}$	Kinetic energy operator
TDDFT	Time Dependent Density Functional Theory
UEG	Uniform Electron Gas
$\hat{V}$	Kinetic energy operator
$\hat{V}_x$	Exchange potential
VASP	Vienna Ab initio Simulation Package (program package)
$\hat{X}$	Electron-electron interaction operator
ϵ_i	Energy eigenvalue
ϵ_{xc}	Exchange correlation energy per electron
ψ_i	Wave function
Ψ	Manybody wave function
∇	Differential operator

Contents

1 Introduction **13**
1.1 Motivation . . . 13
1.2 Basic Concepts . . . 14
1.3 Oxidation . . . 16

2 Copper oxidation **19**
2.1 Earlier studies . . . 19
2.2 Comparison to Al(111) . . . 20
2.3 Oxygen induced reconstruction . . . 22
2.4 Conclusions . . . 25

3 Computational methodology **27**
3.1 Density Functional Theory . . . 28
3.2 Hohenberg–Kohn theorem . . . 28
3.3 The Kohn-Sham ansatz . . . 29
3.4 *Ab initio* molecular dynamics . . . 31
3.5 The dominant approximations . . . 32
3.6 The pitfalls of the method . . . 33

4 Review of the Calculations **37**
4.1 Clean Cu(100) . . . 37
4.2 Oxygen covered and doped Cu(100) . . . 41
4.3 Structurally modified Cu(100) . . . 44

5 Concluding Remarks **49**

Chapter 1

Introduction

1.1 Motivation

Throughout history mankind has always striven to develop more efficient tools with the aim of making our lives easier. Originally the aim was to be able to produce tools of different shape from any material. Nowadays—since we are able to produce almost any imaginable shape from any material—the aim has shifted towards finding better materials for different applications. For example, in electrical engineering, a material that is both conducting and magnetic, yet able to resist corrosion in hostile environments is needed. To create a metal that is inert towards any kind of oxygen-rich acidic environment remains science fiction; however, the gain from such invention makes the subject worth studying.

Why not use coating, one might ask. There are a few simple reasons. Coatings always wear out, and sometimes it is impossible to get the coating to stay on the surface of the material. Characteristics of a coating will always differ from the characteristics of the substrate. This sometimes induces more problems than advantages. Moreover, the most important motivation in the modern world is cost. Coatings are expensive, and in many cases, when the coating wears out, it cannot be replaced. Consequently, a working device may be scrapped due to a failed coating. A good example of this is found in the car industry. In former times the coatings were so poor that the lifetime of the bodies of cars was significantly shorter than that of their engines. Hence, as the body corroded, the working engine was either sold as spare parts, or scrapped together with the body.

In the real world, the shaping of materials is not particularly problematic anymore due to advances in process technology. However, the manipulation of materials at the subnanometer scale by moving individual atoms about is by no means routine even with modern methods. Also, the process itself is so slow that it would be completely impractical to construct highly sophisticated devices that include billions of atoms using such methods. One intriguing way of building such devices would

be a method called self assembly [1, 2, 3], where the atoms organize themselves with only minimal guidance. All the manufacturer need do, is to provide the right environment for self assembly to occur. To achieve this, a good knowledge of atomic scale processes needed to build the device is necessary. Also a deep understanding of the parameters that influence the processes is required. From this point of view, copper is a very attractive material to study, since during oxidation, the oxide forms straight, elongated islands that are only a few atoms wide, and resemble the tracks on a circuit board. The ideal would be to have subnanometer width circuitry grow between individual devices on a chip by self assembly. If one could learn the microscopic reasons behind the elongated growth mechanism then, perhaps, it would be possible to apply the similar principles to grow the metallic interconnect over an oxide layer.
Copper based materials have also drawn interest in the catalysis community due to their low cost compared with other materials possessing similar properties such as palladium or silver. There would certainly be many more applications, if the more expensive metal based oxides could be replaced with lower cost copper based materials. One frequently used example of such devices is the automotive exhaust catalyst. If palladium could be replaced by copper, then at current market prices, the cost of these devices would be about half. Moreover, if it were possible to make catalysts that are more efficient, then proportionately less material would be required, and the cost correspondingly lower.

1.2 Basic Concepts

Any kind of surface reaction begins with the initial deposition of the reactants on the surface. In this case, when considering oxygen, this deposition occurs from the gas phase with some sort of sticking mechanism. The sticking mechanisms in any case can be divided into two different categories: physisorption and chemisorption. In physisorption, the reactants are bound to the surface via a Van der Waals force, which in general is due to the charge distribution in a molecule. This is the dominant force between noble gas atoms. In the case of molecule–metal surface interactions, the Van der Waals force can be considered as the interaction between the incoming molecule and the image charge that it induces within the surface[4]. However, in most situations chemisorption is significantly stronger. This represents chemical bonding between atoms. It occurs by hybridization of the electronic states of the atoms involved in the bonding. It is the most fundamental force that holds condensed matter together at ordinary temperatures. As can be expected, chemisorption plays the central role in most surface processes.
Following their initial deposition, adsorbates can diffuse on a surface to orient themselves to their equilibrium positions, thereby reaching the lowest energy state for the whole system. Diffusion processes can be very complicated, and involve substrate

atoms. On surfaces, diffusion methods vary depending on the favoured adsorption site, and the energetics of transition states. For example, for oxygen, which favours high symmetry sites over substitutional sites, the most probable diffusion method is a jump from one site to another via a lower symmetry site. The process passes through a bridge site, which represents the transition state.
From a computational point of view, it is convenient to define a few parameters which indicate the reactivity of the surface and the stability of the adsorbed overlayers. One such parameter for surface reactions is the adsorption energy E_{ads}, which represents the energy difference between the initial undeposited state and the final adsorbed state energies.

$$E_{\mathrm{ads}} = E_{\mathrm{total}} - E_{\mathrm{slab}} - E_{\mathrm{init}}, \tag{1.1}$$

where E_{total} is the total energy for the system consisting of the adsorbate in its adsorbed state and the surface slab, E_{slab} is the total energy for the surface slab, and E_{init} is the total energy for the initial state for the adsorbate (in the case of oxygen, the gas phase spin triplet state).
For oxygen adsorption this represents the energy difference between the gas phase state and various final state configurations. Another useful quantity that is considered throughout this work is the dissociation energy E_{dis}. It measures, the energy required to dissociate an oxygen molecule in a given configuration. It is defined as the energy difference between the molecular adsorption state and the maximum energy state on the minimum energy pathway towards the dissociated state:

$$E_{\mathrm{dis}} = E_{\mathrm{TS}} - E_{\mathrm{s_{max}}}, \tag{1.2}$$

where E_{TS} is the transition state energy. Usually, this is the molecular adsorbed state on the surface (precursor state). $E_{\mathrm{s_{max}}}$ is the maximum bond stretching energy for the oxygen molecule corresponding to the transition state.
To describe surface reactions, the present method is to calculate the potential energy surface (PES). This is a mapping of the energetics of the reaction under study. A PES contains all the information concerning a reaction with a full description of the energetic states including the vibrational modes of the reactants, and the different adsorption states. Since it carries so much information, the complexity of the PES increases directly with the allowed degrees of freedom in the system. In surface reactions, when calculated without any approximations, the PES contains all the degrees of freedom of the surface atoms as well as the adsorbent. When expressed in this form, it is impossible to handle. However, the number of the degrees of freedom can be reduced by making some approximations. For example, when the surface atoms are neglected, the PES for O_2 adsorption on any surface reduces to only six dimensions. These dimensions are the centre of mass coordinates of the O_2 (x, y, z), the bond length d, and the angles of the molecule with respect to the surface (Θ, Φ). This approximation is valid given that the surface atoms are relatively immobile and

that the adsorbents are several times lighter than the substrate atoms. Naturally, information about the heat transfer between the adsorbent and the surface is lost when using this approximation. To visualize the PES, two-dimensional cuts of the six-dimensional PES are used. See Fig. 1.1 showing some features that can be used to characterize the adsorption process.

1.3 Oxidation

The rapid development of theoretical and experimental methods in surface science has made it possible to study increasingly complex systems. Surface reactions occuring on timescales too short to be investigated experimentally are of particular interest here. During recent years, oxidation of transition metals has become a subject of intense research activity, owing to the fact that in many catalytic reactions it has been shown that the rate limiting step of reactions is the oxidation of the substrate materials [5, 6]. Moreover, the catalytically reactive part of the substrate material is in many cases the oxide film rather than the substrate itself [7]. Thus, knowledge of the fundamental reactions involved is needed to achieve control over more complex reactions. This enables materials to be developed that have superior properties over those used for catalysts and corrosion resistant materials at present. These properties are not completely exclusive. Ideally, a good catalyst should have strong reactivity towards dissociation of O_2, while having only weak binding towards oxygen atoms, thereby making the atoms available for subsequent reactions with other constituents. In the case of corrosion resistant materials the key factor usually is the fact that the surface should be repulsive towards gas phase oxygen. For example, in the case of aluminium, the oxidation process creates an oxide film that acts as a protective coating over the substrate. The oxygen atoms bound to the surface repel oxygen atoms in the gas phase, thus inhibiting further oxidation of the surface. In many other metal surfaces, the growth of the oxide film over the substrate weakens the binding energy of the oxygen atoms, increasing the catalytic involvement of the on-surface oxygen in other reactions such as CO oxidation [7]. For example, it occurs for the low temperature water-gas shift [8, 9, 10], where hydrogen is extracted from water in the vicinity of copper surfaces. Similar weakening of binding energies is demonstrated in this work for copper.

In materials science, theoretical investigations are now regarded as being essential. In many instances experiments yield results that lack explanation without detailed knowledge of the electronic structure of the system. No method is able directly to probe the electronic states of any material experimentally without influencing the measured system. Thus, the ability of computational methods to access to detailed information about electronic structure provides the only means by which full understanding can be achieved. Progress in the development of these methods permits increasingly complex systems to be investigated. Certain limitations remain; how-

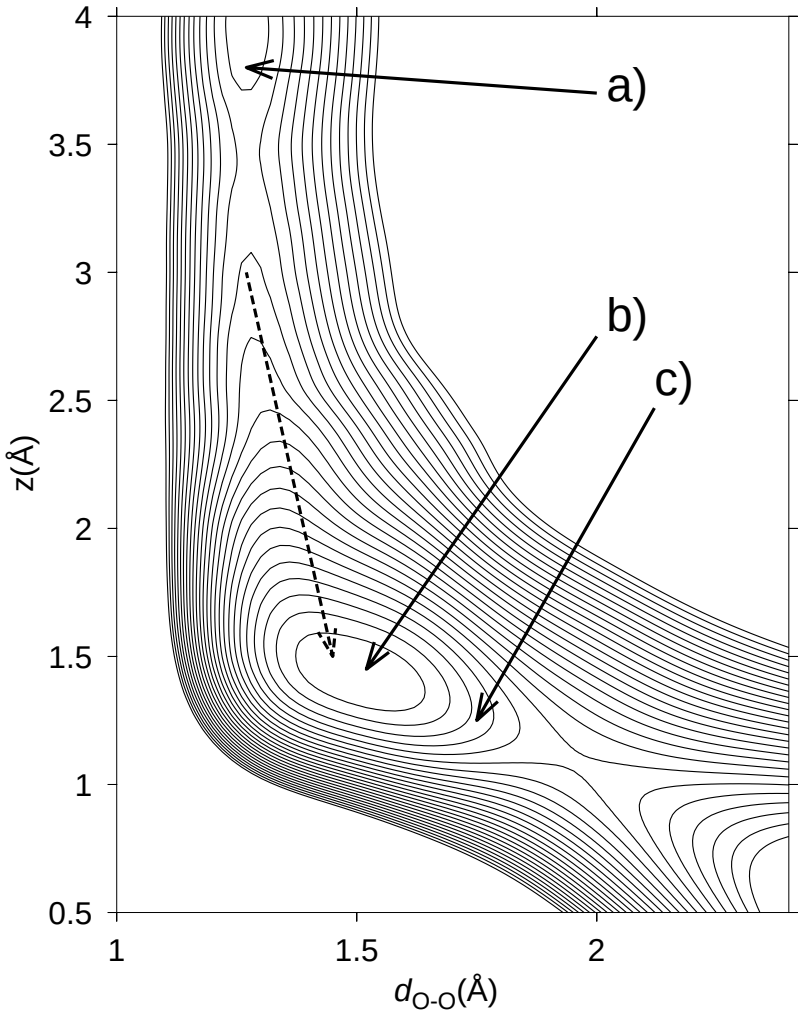

Figure 1.1: Example two-dimensional cut through the six-dimensional PES, showing in the form of a potential-energy contour map, many features typical for the adsorption of diatomic molecules. The horizontal axis represents the intra molecular bond-length, and the vertical axis represents the molecular centre of mass distance from the surface. (a) shows the entrance channel, which in this case possesses a small barrier; (b) shows the molecular adsorption state close to the surface; (c) presents the late barrier at the exit channel. The kinetic energy gain is marked with the dashed line between the entrance channel and the molecular adsorption state.

ever, provided sufficient care is taken, it is usually the case that computer simulations provide good results. Moreover, when good agreement is achieved between simulation and experiment, the additional detailed information provided by theory—such as the entire quantum mechanical description of the system, including the wave functions for each valence electron—is likely to be reliable. The value of this information is high. For a chemical reaction on the surface—which usually occurs so quickly that even measuring the atomic positions near the transition state is at best difficult, and more likely impossible—obtaining information experimentally about changes in the electronic structure during dissociation is completely prohibited by the Heisenberg uncertainty principle.

In the present study an *ab initio* formalism is employed to gain insight into the early states of oxidation reaction on a Cu(100) surface. The main calculations are performed for clean Cu(100) surfaces. These are compared with modified and oxygen precovered surfaces, and stepped Pd(211) and Cu(211) surfaces. The methods used throughout are essentially 'standard' in the surface science community. However, several ways to apply the techniques to gain more reliable results are also proposed, together with ones that are not yet established.

Chapter 2

Copper oxidation

2.1 Earlier studies

The initial oxidation of Cu(100) has drawn much attention, both experimental and theoretical. The first thorough attempt to explain the oxidation of metal surfaces was made in 1948 by Cabrera and Mott [11], who where able to provide a satisfactory description of the oxidation process. They studied metal surfaces, as well as bulk-oxide formation, and thin oxide film formation in this extensive study. The main conclusion of their work is that during oxide formation, the oxygen pulls metal atoms through the thin oxide film; thus, the oxide continues to grow. Although the results are good and the explanation is reasonable, it has a some serious drawbacks. First, they give no explanation for the initial stages of the oxygen sticking on the surface, which has so far shown to be the rate limiting step in many catalytic processes, as well as for the oxide formation itself. Secondly, they assumed a uniform oxide growth. Often this is not a valid approximation. For example, in the case of Cu, the oxide layer exhibits considerable inhomogeneity even on single crystal surfaces, as will be discussed later. To understand the reasons for this lack of information, one has to put the study into perspective. Since the 1940s there has been considerable development in experimental techniques. Nowadays it is almost routine work to reach the atomic scale even with *in situ* equipment. This has enabled the study of many surface processes in the level of detail that was not accessible those days. Another pioneering work—which demonstrates the central role which copper has played in surface science—is by Lawless and Mitchell [12] in the 1960s. They suggest that the first Cu layer is first saturated with oxygen, and only then the oxide formation begins. Most of their results remain in excellent agreement with many present-day studies.

Later, there have been several ambitious attempts to find the parameters that affect the adsorption of any dimolecular species on a metal surface. One of the most successful explanations is probably the *d*-band model by Hammer and Nørskov [13],

which states that the centre of the *d*-band, i.e. the chemical potential of the surface, determines the reactivity. This model successfully explains the nobleness order of the metals, but being such a simple model, it cannot take into account the geometrical aspects. Moreover, the distance of the center of the *d*-band from the Fermi level is not unambiguously determined. For example, in lower coordinated sites, the *d*-band is usually higher in energy, which suggests higher reactivity, as it should. However, in general, lower coordination does not always mean higher reactivity. A good example of this is Cu. The (110) surface has the lowest coordination among the low index surfaces, but is less reactive than the higher coordinated (100) surface [14].
It is well established experimentally that the initial sticking of O_2 on Cu(100) [15, 16, 17] follows type-I Langmuir dynamics [18], which is usually associated with direct activated dissociative sticking. Here, the approaching molecules will either directly dissociate by overcoming the energy barrier associated to the sticking process, or scatter back to the gas phase without sticking. This implies that there is a potential energy barrier, which the molecule must overcome before sticking to the surface. From a theoretical viewpoint, this means that the upper part of calculated Potential Energy Surface (PES) plots should exhibit a barrier, corresponding to an entrance channel. However, in this case, theoretical results have not shown any indication of such barriers [19].

2.2 Comparison to Al(111)

Molecular Beam Surface Scattering (MBSS) experiments for O_2 on Al(111) shows dynamical behaviour similar to that for O_2 on Cu(100) [20]; however, their calculated PES's exhibit no such features. The discrepancy remained unexplained for years until 2004 when Behler *et al.* [21] performed a thorough investigation. The cause of the discrepancy was identified as being due to the adiabatic approximation used in the calculations, and the fact that the different spin states of oxygen are poorly described by present exchange-correlation approximations [22]. In the chemistry community it is a well known fact that molecules which have a spin triplet ground state are very inert towards any substrates with singlet configuration, due to spin momentum conservation rules. The spin relaxation from the triplet state to the singlet state—which is required as the molecule approaches the surface—occurs over similar time scales to the adsorption process itself. This causes an additional spin friction effect, which alters the adsorption dynamics [22], essentially by increasing the adsorption barrier, and consequently decreasing sticking. Binetti *et al.* reported a semiquantitative agreement between theoretical and experimental results. The agreement was achieved by taking into account nonadiabatic effects [23]. The same study also found that molecular rotations inhibit sticking: parallel relative alignment of the incoming molecules is favoured over vertical ones, meaning rotating molecules are more likely to miss the cone of acceptance.

It is likely that these effects will have a similar influence on O_2 interactions with Cu(100), owing to their close relationship. However, before making such conclusions this must be demonstrated. Thus, it represents the initial motivation for the present work. Moreover, spin relaxation and molecular rotations only influence the initial sticking behaviour: a full understanding of the early stages of oxidation also involves what happens immediately afterwards. A detailed examination of this is conducted in this work as well.

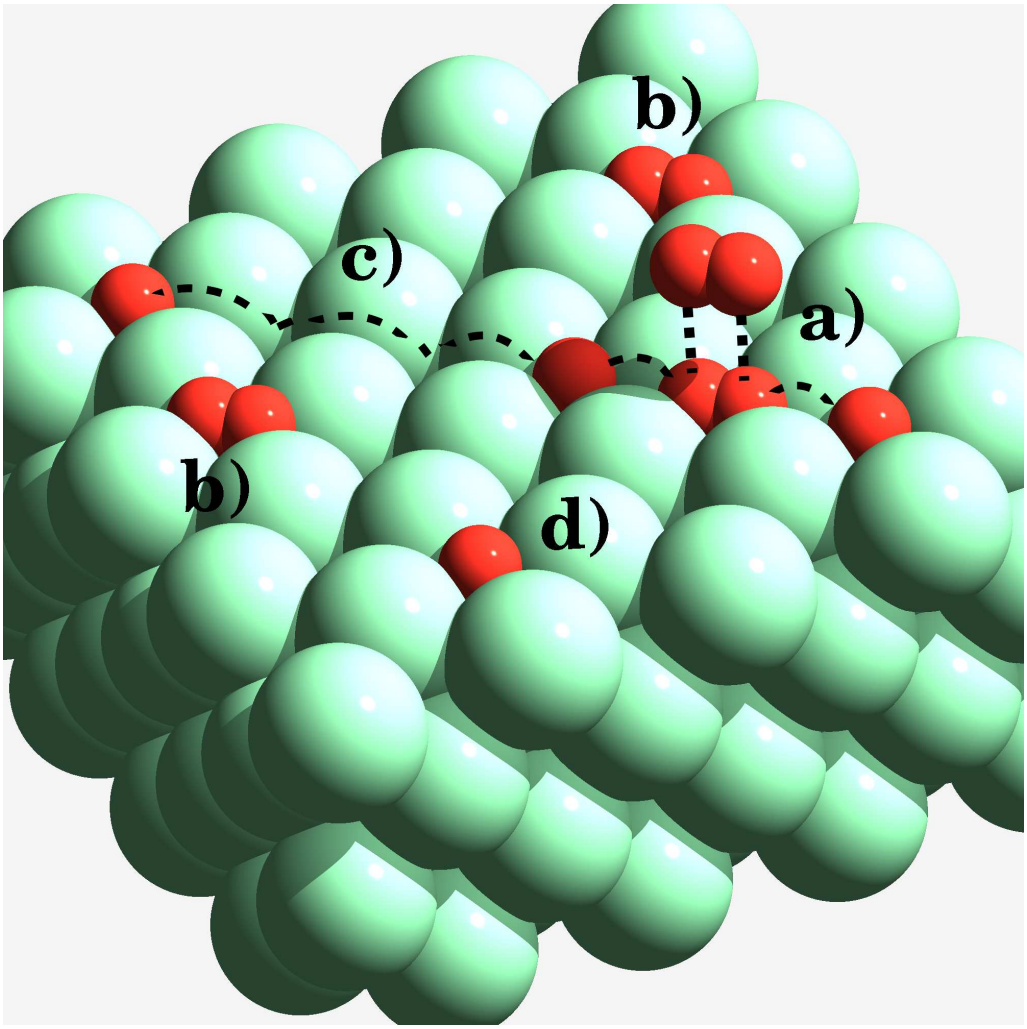

Figure 2.1: The initial adsorption: a) direct dissociation, b) molecular adsorption, c) "hot" atoms travelling ballistically through the surface with the energy gain from the dissociation, and d) atomic adsorption.

In a recent study employing Monte Carlo simulations [24], it was pointed out that, in general, the chemisorption of O_2 on any {100} surface inevitably occurs by type-I Langmuir adsorption, where the surface oxygen coverage depends on the gas pressure, when the direct adsorption mechanism dominates over the indirect one. A typical feature for this kind of adsorption is the formation of disordered $p(2 \times 2)$

and $c(2 \times 2)$ overlayers (Fig. 2.2). In the other case—where the indirect pathway dominates—the corresponding ordered phases are formed. Oxygen on Cu(100) surface initially forms a locally ordered structure [25]; however, the the local ordering can be due to the high mobility of the surface [26, 27]. Therefore, any conclusions drawn about the chemisorption mechanism should bear this in mind.
A Monte Carlo study by Jaatinen *et al.* [28] revealed that two dimensional adsorbate ordering occurs due to the interaction energetics regardless of the adsorption dynamics. This is an indiction of the fact that the diffusion rate on a Cu(100) surface is so high that the adatoms on the surface are not affected the way in which they initially were deposited before forming a structure. Moreover, kinetic energy that is freed during the dissociation process also contributes to the local or global order of the adsorbate layer. It is shown that it gives the dissociated atoms lifetimes up to 0.5 ps before the actual chemisorption [29] (see Fig. 2.1). There is also experimental evidence of these so called "hot" adatoms being able to travel ballistically through the surface before chemisorption occurs [30]. However, these results are not currently supported by any theoretical calculations, and the conclusions are based more on hypotheses, rather than direct observations.

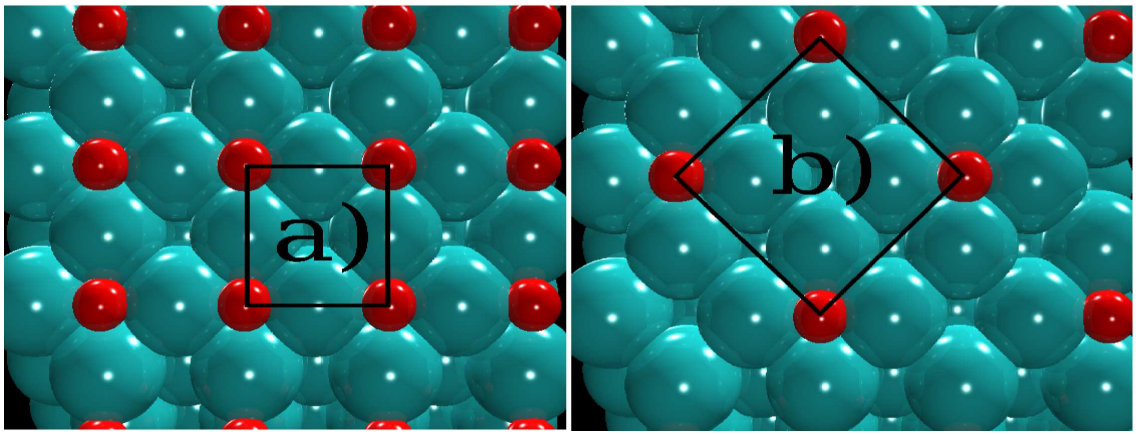

Figure 2.2: Adsorbate ordering on Cu(100) surfaces at low coverages. a) $c(2 \times 2)$ b) $p(2 \times 2)$ structures corresponding to coverages 0.25 ML and 0.5 ML. The $c(2 \times 2)$ structure is stable only in small islands and low temperatures cause by restructuring of the surface owing to the minimization of the adsorbate induced strain (see text).

2.3 Oxygen induced reconstruction

Experimental investigations have shown features that are typical for the oxidation of Cu(100) and only a few other metal surfaces. Probably the most interesting ones—in the sense that they dominate the oxide growth later on—are the surface

reconstructions known to occur on {110} and {100} facets of Cu. The {110} surface reconstructs with (2×1) symmetry [31, 32, 33, 34], whereas the {100} surface has a somewhat more complicated, almost completely ordered $2(\sqrt{2} \times \sqrt{2})R45°$ structure [35, 36] (see Fig. 2.3). The dominant feature of the reconstruction is the missing Cu atom row between the four fold sites occupied by the oxygen atoms. The phase is complete when the oxygen concentration on the surface exceeds a threshold concentration of 0.5 ML [36]. This reconstruction is not entirely unique for Cu(100). A similar structure is also observed for O/Ag(100) [37] differing from the reconstruction on O/Cu(100) only by the relaxation of the substrate and adsorbate atoms. Moreover, the structure predicted by *ab initio* calculations is identical for both materials [38], showing that the effect is caused by a phenomenon which is available on both surfaces. On Cu(100), at the same time as this structure forms, the sticking behaviour of oxygen molecules changes from direct activated dissociation to a non-activated process, with features that are typical for a precursor mediated process, with thermal activation involved. This is discussed in publication IV, based on the present theoretical results.

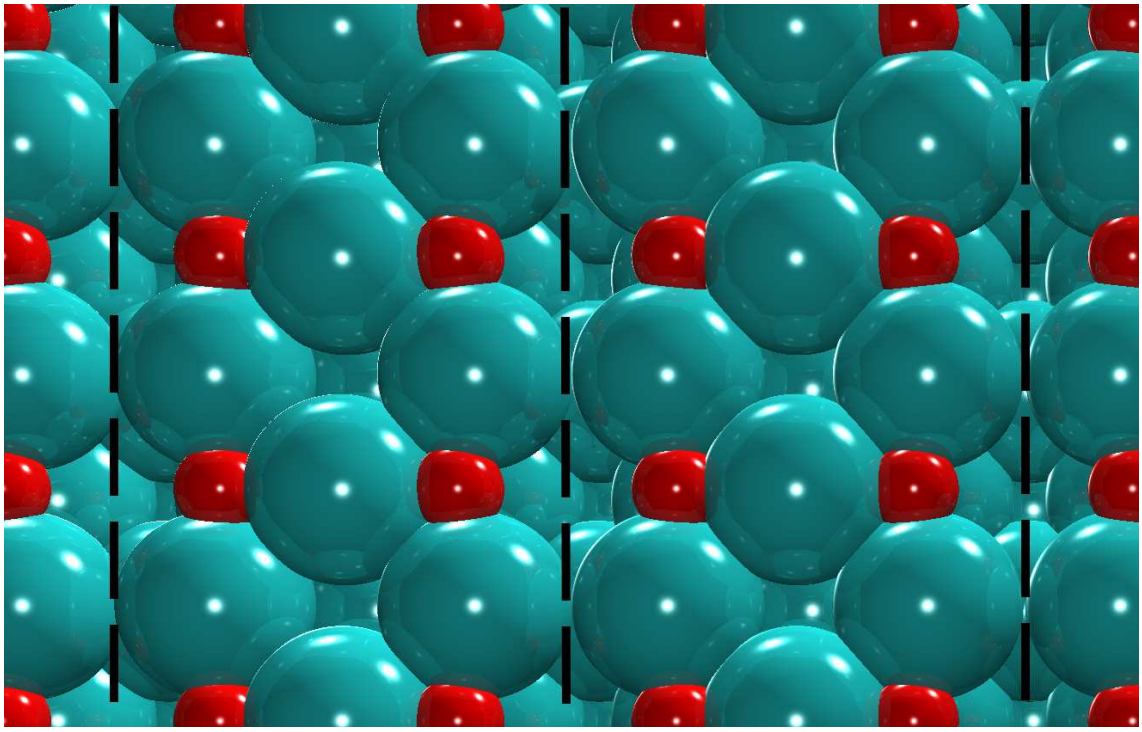

Figure 2.3: The missing row $2(\sqrt{2} \times \sqrt{2})R45°$ reconstruction on Cu(100), which is formed to minimize the Coulomb lattice energy after 0.34 ML oxygen coverage. The dashed black lines indicate the missing Cu row. The oxygen atoms have relaxed away from the missing row to maximize the distances both to the other oxygen atoms, the unsaturated Cu in the middle.

The driving force for the structural reconstruction of the surface is the minimization

of the Coulomb lattice energy. The following explanation for the phenomenon was developed by Stolbov *et al.* [39, 40] using first principles methods. For both Ni(100) and Cu(100), the oxygen atoms occupy the same four-fold sites; hence, both surfaces should have the same $c(2 \times 2)$ structure at the saturation concentration. When the oxygen atoms adsorb to metal surfaces they tend to charge negatively, due to their electronegativity. This causes oxygen-oxygen Coulomb repulsion for the adsorbents. According to Stolbov *et al.*, the reason for Cu(100) undergoing reconstruction and Ni(100) not, is that despite the fact that in both cases there is a strong Coulomb repulsion between the oxygen atoms, in the case of Ni(100) the repulsion is effectively compensated by the strong bonding between the pO-dNi orbitals. In contrast, the bonding between the pO-dCu orbitals is weaker, and insufficient to prevent the reconstruction from occuring. Thus, the Coulomb lattice energy is minimized by the reconstruction on Cu(100) by maximizing the distance between the oxygen atoms.
Reconstruction dynamics has been addressed experimentally by Jensen *et al.* [41]. Scanning Tunneling Microscopy (STM) was employed. The experiments showed that the adsorbed oxygen atoms first form a disordered structure before the onset of reconstruction. Moreover, the surface first is roughened by the adsorption energy of the incoming molecules (1.4 eV), which is larger than the Cu-Cu bond breaking energy (0.3 eV). Once vacancies are created, roughening the surface, the reconstruction occurs locally. However, the broken Cu bonds are so far apart that the reconstruction is unable to proceed further. As the oxygen coverage increases, the distance between the broken bonds decreases. This gives the possibility for the reconstruction of the surface to proceed in a collective fashion to its lowest energy state. Recently, Harrison *et al.* [42] found evidence that reconstruction relieves adsorbate-induced surface stress. Their investigation employed a crystal curvature technique in conjunction with density functional theory based calculations. Adsorption of oxygen into the $c(2 \times 2)$ structure was shown to generate more compressive stress in the surface than the $2(\sqrt{2} \times \sqrt{2})R45^\circ$ structure by both theory and experiment. Based on the previous arguments, it can be concluded that the driving force which induces the reconstruction is minimization of the Coulomb lattice energy, and consequently lowering of the surface stress.
The next phase in the oxidation process is the initial growth of oxide islands over the reconstructed phase [36]. In one of the first atomic resolution *in situ* measurements for Cu(100) by Yang *et al.* [43], it was found that the main oxide growth mechanism on this surface is the surface diffusion of the oxygen atoms, and that the oxide growth is three dimensional. In the same investigation, a direct dissociative sticking mechanism from the surrounding gas phase was also observed.
In 2002, experiments by Zhou *et al.* [44], found elongated oxide islands growing epitaxially, aligned along either (001) and $(00\bar{1})$ or (010) and $(0\bar{1}0)$ when a Cu(100) surface is oxidized at 600°C. Initially the islands are square shaped; however, once the size grows above a critical dimension of 110 nm, elongation begins. These elon-

gated islands have shown to be a promising basis for self assembling nanowires, since their size and shape can be controlled by modifying the environmental parameters of the oxidation process, and the surface morphology [36]

2.4 Conclusions

Based on existing evidence, the process of Cu(100) oxidation can be represented by a simple block diagram (Fig. 2.4). It begins with the initial deposition of O_2 molecules on clean Cu(100). The adsorption mechanism is dissociative adsorption. The oxygen adsorbs in the four fold sites on the surface, and repulsion between the oxygen atoms causes the $2(\sqrt{2} \times \sqrt{2})R45°$ reconstruction. As the oxidation continues, elongated nanosize oxide islands start to form over the reconstructed area. Following long exposure, the surface is filled with the growing oxide islands, until finally the whole surface is oxidized.

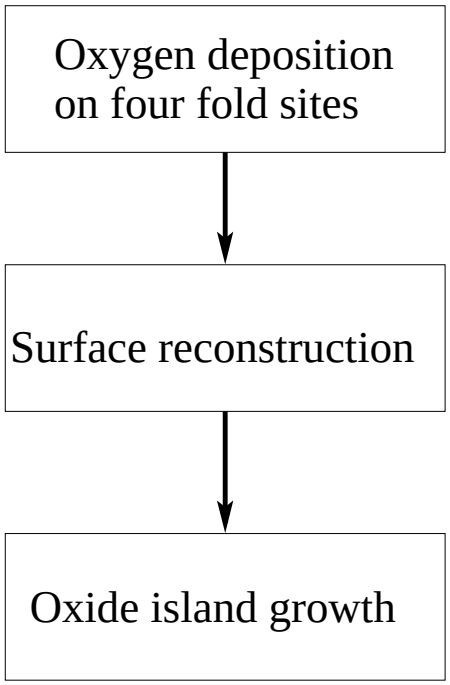

Figure 2.4: Schematic diagram showing the oxidation of Cu(100) surface.

As the figure and the preceding review illustrate, the understanding of the process is only qualitative, and the details of the processes involved are mostly missing. The aim for this project is to concentrate on the details, and give information about the early stages of the process.

Chapter 3

Computational methodology

Most of the calculations presented in this thesis are performed using the Spanish Initiative for Electronic Simulations with Thousands of Atoms (SIESTA) [45, 46] program package. The fundamental idea behind the SIESTA formalism is to use localized orbitals of different symmetry to describe the wavefunctions of the electrons rather than using a planewave basis [47, 48, 49]. The advantage of this approach compared with planewave based calculations is the fact that the basis functions have a set radial cutoff distance above which they vanish. Thus, for example, the empty space in a supercell is not filled with wavefunctions that are essentially unoccupied. This reduces the computational demand especially in surface calculations, where the amount of empty space in a supercell is typically more than half of the total volume. In this chapter the applied methodology and the pitfalls associated with it are discussed. First, an introduction to the basics of density functional theory are described. This is followed by a discussion of the necessary approximations employed. Finally, some pitfalls involved in applying the methodology are examined. To validate the performance of pseudopotentials and basis sets used in SIESTA calculations, some of the configurations are also calculated using Vienna Ab-initio Simulation Program (VASP) [50, 51, 52, 53]. It employs Projector Augmented Wave (PAW) [54] potentials, and planewave basis functions. PAW potentials can be considered as being nearly equivalent to all electron methods, owing to the fact that, in principle, it is possible to reconstruct all electron wavefunctions by using the PAW method. These facts make it a good checkpoint for the more approximate, but much faster SIESTA method. Within both methods, the Monkhorst-Pack [55] is used to sample the Fourier space in the first Brillouin zone. The density of the mesh depends on the problem. This is reported in each of the Publications. Using a special k-point mesh provides the same quality of results as a homogeneous sampling, while requiring fewer k-points, thereby reducing the computational burden. The advantage of using a homogeneous sampling is that the total energy converges systematically with the number of k-points. This is not necessarily the case with a special mesh. Therefore, more thorough testing is required. Especially for bulk

metals, where many k-points are needed, the advantages of using a Monkhorst-Pack mesh instead of a homogeneous mesh is less pronounced, and controlling the energy convergence with respect to k-point mesh is easier with a homogeneous mesh [56].

3.1 Density Functional Theory

This section describes the underlying theoretical formalism upon which this work is based. Density functional theory (DFT) [57, 58] is founded on the notion that a quantum mechanical system can be expressed as a functional of its electron density in the ground state. DFT was originally developed in two parts, namely the Hohenberg-Kohn theorem, and its practical implementation in the form developed by Kohn and Sham. Without the latter, the first theorem would probably have remained merely a curiosity.

3.2 Hohenberg–Kohn theorem

The formulation begins by stating that the total energy of a many-body system (Schrödinger equation) is

$$H\Psi = E\Psi. \tag{3.1}$$

Here, Ψ is the many-body wave function, and H is the Hamiltonian for the electrons in an external potential including fixed nuclei:

$$H = -\frac{\hbar^2}{2m}\sum_i \nabla_i^2 + \sum_i V_{ext}(\mathbf{r}_i) + \frac{1}{2}\sum_{i\neq j}\frac{e^2}{|\mathbf{r}_i - \mathbf{r}_j|}. \tag{3.2}$$

This can be expressed in an operator form,

$$\hat{H} = \hat{T} + \hat{V} + \hat{X}, \tag{3.3}$$

where $\hat{T}$ is the kinetic energy operator, $\hat{V}$ is the external, or ionic, potential, and $\hat{X}$ includes the electron-electron interaction. The first two terms are relatively straightforward to deal with since they include only Coulomb terms. However, the last one is more problematic, as will be shown later.
When the Hamiltonian is substituted into the Schrödinger equation, it takes the form

$$(\hat{T} + \hat{V} + \hat{X})|\Psi\rangle = E|\Psi\rangle. \tag{3.4}$$

There is set $\mathbf{V}$ of one-particle potentials for which all $\hat{V} \in \mathbf{V}$; hence, the previous operator equation implies a non-degenerate ground state energy exists for the many-body problem. When a set of all ground state wave functions is expressed as Ψ the

Schrödinger equation defines a function $\sigma : \mathbf{V} \rightarrow \mathbf{\Psi}$. A fermion density operator with $\hat{n} \in \mathbf{N}$, which is the sum of one particle densities, is then introduced as

$$\hat{n}(\vec{r}) = \sum_i \psi_i^*(\vec{r})\psi_i(\vec{r}). \tag{3.5}$$

It expresses the ground state density in terms of the many-particle wave functions, $\Psi \in \mathbf{\Psi}$,

$$n(\vec{r}) = \langle \Psi | \hat{n}(\vec{r}) | \Psi \rangle. \tag{3.6}$$

This also defines a function that derives the densities from the wave functions, $\rho : \mathbf{\Psi} \rightarrow \mathbf{N}$. Both of these functions are bijective and together constitute a mapping from the ground state wave functions to the ground state densities ($\sigma^{-1}\rho^{-1} : \mathbf{N} \rightarrow \mathbf{V}$). This is an important result, since it shows that it is possible to define the electron density as being the principal variable, upon which all other variables depend, and use it instead of the wave functions. However, one term remains in the Schrödinger equation, $\hat{X}$, which is not properly defined.

3.3 The Kohn-Sham ansatz

Although the Hohenberg-Kohn theorem provides the foundation of density functional theory by showing that the ground state electron density can be used as the principle variable, it provides no means for calculating the density; the formalism developed by Kohn and Sham achieves this. The derivation of the Kohn-Sham equations [58] begins from the functional expression for the charge density $n(\vec{r})$ in a static potential $v(\vec{r})$.

$$E[n] = \int v(\vec{r})n(\vec{r})d\vec{r} + \frac{1}{2}\int\int \frac{n(\vec{r})n(\vec{r}')}{|\vec{r} - \vec{r}'|} d\vec{r}d\vec{r}' + G[n], \tag{3.7}$$

where the energy functional $G[n]$ can be expressed as

$$G[n] = T_s[n] + E_{xc}[n]. \tag{3.8}$$

In equation (3.8) $T_s[n]$ represents the kinetic energy of the noninteracting system, and E_{xc} the exchange-correlation term. The exchange-correlation term is fully quantum mechanical, and represents the effects that in an interacting system are due to the fact that electrons tend to avoid each other. Therefore, there is a lowering of the electron density in the vicinity of each electron. This is usually called the exchange-correlation hole [59]. Moreover, the E_{xc} term includes also the kinetic energy of the interacting system that is not included in the non-interacting case, together with the additional complication of $T_s[n]$ being a function of the charge density of the

interacting electron system. This conundrum is resolved as follows.
For N interacting particles, the ground state density can be expressed in terms of the ground state wave functions

$$n(\vec{r}) = \sum_{i=1}^{N} \psi_i^*(\vec{r})\psi_i(\vec{r}). \tag{3.9}$$

The one electron Schrödinger equation takes the form

$$(T[n] + V_{eff}[n])\psi_i = \epsilon_i \psi_i, \tag{3.10}$$

where the effective potential V_{eff} consists of the electrostatic potentials of the ions and electrons—or the Hartree potential—and the exchange-correlation potential. The other potentials can be explicitly defined, but the functional form of the exchange-correlation potential is unknown. However, a series expansion for the potential can be made, and provided a slowly varying potential is assumed, second and higher order terms of the potential can be neglected. This method is called local density approximation (LDA), or local spin density approximation (LSDA) in the spin polarized case.
Following the notation in [58], the LDA can be expressed as

$$E_{xc}[n] = \int \epsilon_{xc}(n) n d\vec{r}, \tag{3.11}$$

where ϵ_{xc} is the exchange-correlation energy per electron in a uniform electron gas (UEG). In practise the exchange-correlation potential is parametrized to reduce the computational burden. The most frequently used parametrization is that by Ceperly and Alder (CA) for the UEG on the basis of their Monte-Carlo calculation [60]. Although the approximation seems crude at first sight, it works well in many applications. However, there are several systems, where this method cannot be applied. The approximation fails in systems which include strong electron correlation, such as transition metal oxides or some semiconductor systems. Situations where density gradients are significant such as surfaces are also poorly described.
Many ways of improving the LDA have been proposed. Currently, the most practical in terms of computational cost versus accuracy, is the Generalized Gradient Approximation (GGA), where density gradients are included. Owing to the way that the gradients can be described being not unique, there are several ways of constructing gradient corrections; however, none of them appear to be universally applicable. GGA functionals are justified by their empirical success rather than than on physical grounds. In pr actice for surfaces, the GGA has proven to be a better approximation than LDA. In the present work, the Perdew-Burke-Ernzerhoff (PBE) [61] formulation is employed within the SIESTA program package. It is op-

timized to give results similar to the Perdew-Wang 91 (PW91) [62] GGA that are used in the VASP package.
An improved way of calculating the exchange-correlation contribution to the total energy is to take a selected fraction of the exact exchange contribution, calculated using Hartree-Fock method, and mix it with GGA exchange term, taking the correlation part from the GGA potential (hybrid potentials). To do this, the exchange and correlation parts of the potential must be separable. The exchange potential can thus be calculated exactly according to Hartree-Fock theory using Kohn-Sham orbitals [63]:

$$\hat{V}_x = -\frac{1}{2}\sum_{i,j}\int\int d\vec{r}d\vec{r}'\frac{e^2\delta_{s_i,s_j}}{|\vec{r}-\vec{r}'|}\psi_i^*(\vec{r})\psi_i(\vec{r}')\psi_j^*(\vec{r}')\psi_j(\vec{r}). \tag{3.12}$$

Here, s_i and s_j represent the spin states of electrons labelled i and j.

3.4 *Ab initio* molecular dynamics

Throughout this work, static PES calculations are complemented with first principles molecular dynamics calculations. The dynamical calculations employ the adiabatic approximation. First, the electronic structure is calculated for the initial atomic coordinates. From this it is possible to calculate the forces acting on each atom using the Hellman-Feynmann theorem [64],

$$F = -\frac{\partial E}{\partial R_i}, \tag{3.13}$$

where E is the energy, and R_i is the coordinate of atom i.
The dynamical problem can subsequently be solved by integrating Newton's second law,

$$F = ma, \tag{3.14}$$

where m is the atomic mass of the nucleus and a is the acceleration.
Forces are calculated once at every time step. The duration of the time step must be sufficiently short to prevent aliasing of the highest frequency molecular vibrations. This is determined by the Nyquist theorem,

$$f_s > \frac{f_{\max}}{2}, \tag{3.15}$$

where f_s is the sampling frequency, and $f_{\max}$ is the maximum molecular vibration frequency. In pr actice, the sampling frequency must be at least ten times larger than the Nyquist frequency so that kinetic energy is conserved properly.
If the electronic problem is solved at each time step, independently from the nuclear

motion, then adiabatic behaviour for the system is assumed. This means that the electronic structure remains at the ground state throughout the simulation. There are some processes in which the electronic structure does not remain at the adiabatic ground state, and hence electronic excitations occur (see next section for details). It is possible to escape from the adiabatic surface in MD simulations by propagating the Schrödinger equation simultaneously with the atomic coordinates [65]. This method is called Time Dependent Density Functional Theory (TDDFT) [66]. There are several implementations of this kind of approach; however, the best way to propagate Schrödinger-like equations is unknown [67]. Existing methods provide accurate simulations of optical transitions, but have problems with atomistic molecular dynamics.

3.5 The dominant approximations

The main approximation involved in performing structural optimizations is the adiabatic, or Born-Oppenheimer (BO) approximation [68]. Within this approximation the assumption is made that electrons and nuclei—owing to the difference in their masses—move at rates which are on such different timescales that the electrons respond instantaneously when the atomic coordinates change on each MD step. Thus, the approximation is adiabatic in the sense that the electronic system is always in its ground state with respect to the nuclear positions. For most systems this approximation is well justified. However, if for some reason the system restricts the movement of the electrons from one state to another with some additional friction-like component (for example the spin selection rules discussed in chapter 2 for O_2 on Al(111)) or the ions are moving at high velocity, then the approximation is no longer valid, owing to the fact that the system has deviated significantly from an equilibrium state.

In the present calculations, the core electrons are described using the pseudopotential approximation. It is based on the idea that most of the chemical properties of matter are determined by the valence electrons. Electrons closer to the core are chemically inert. The approximation can be justified on the basis that the core electrons are tightly bound to the nuclei compared with the valence electrons. Thus, they participate relatively little in chemical phenomena such as charge transfer or bonding. These higher energy states also posses rapidly varying wavefunctions; hence, they impose a relatively large computational burden owing to needing either more basis functions (planewave method), or requiring a denser integration mesh (local orbital method) than do the valence electrons. By replacing the chemically inactive core electrons with an ionic potential that represents their net effect, the pseudopotential approximation greatly simplifies the problem.

In this work, the pseudopotentials are of Troullier-Martins [69] type. They are norm-conserving potentials, meaning that outside a given core region (Fig. 3.1), the

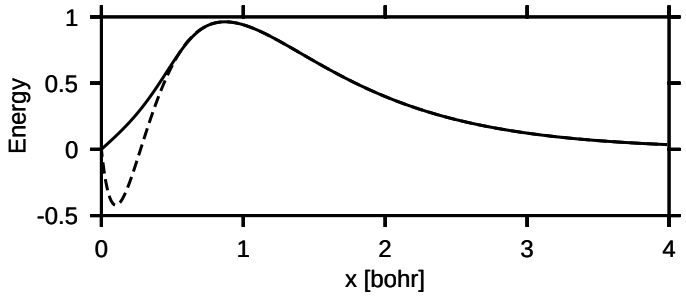

Figure 3.1: The pseudopotential for the $2s$-orbitals of an oxygen atom used in the present calculations. The dashed line represents the all electron wave function. Note that due to the norm-conservation constraint, beyond the core radius the all-electron and the pseudo-wavefunctions are equal. The horizontal axis represents the distance from the atomic centre.

all-electron potential and the pseudopotential are identical; hence, yield the same charge density. This improves the transferability of pseudopotentials even between different chemical environments. Usually, a separate potential is constructed for each angular momentum component to achieve this. The pseudopotentials employed here follow this scheme. For Cu, the valence configuration $3d^{10}\,4s^1$ is used, with orbital cut-off radii of 1.58 and 2.03 Bohr, respectively. This is a steep pseudopotential, but since the system also contains oxygen atoms, the cut-off radius for the oxygen $2p$-orbital represents the limiting factor. For O the valence configuration $2s^2\,2p^4$ is used, with the corresponding orbital cut-off radii of 0.87 and 0.81 Bohr. Closely related to pseudopotentials is the approximation for the exchange–correlation term. As was previously described, in this work the GGA is applied.
Another crucial approximation used is the basis set and its quality. By far the most popular basis set used in electronic structure calculations is a plane wave basis. This is a natural choice, due to the solutions for wavefunctions in periodic potential being, according to the Bloch theorem, modified planewaves [70]. However, in the case of surface calculations, this basis set has one major disadvantage. This arises from the fact that, while using a planewave basis, the vacuum region necessary to create the surface, is also filled with planewaves that only represent empty space. To avoid this, localized basis sets, consisting of either Gaussian functions, or numerical atomic orbitals (NAO) can be used. The present calculations utilize the latter type [48].

3.6 The pitfalls of the method

The main errors in calculations arise from inadequate descriptions of the core potentials, i.e. poor pseudopotentials. The transferability of pseudopotentials, no matter

what type is used, is always questionable. It is rather disturbing that currently in the materials science community, pseudopotentials are usually used without investigating their applicability in a given situation. There are several examples, where it has been shown that a discrepancy between theory and experiments can be traced down to poor pseudopotentials [71] or inadequate description of the ion cores.
Given computational resources are inevitably finite, it is also a tempting idea to lower the computational burden by simply using a smaller basis set for the wavefunctions. This is not a bad idea, provided convergence of the results is guaranteed. However, in many instances, there is no way of knowing this before doing the same calculation with the reduced basis and the full basis. This is especially a problem for the localized orbital methods, due to the fact that required extents and sizes of the basis may vary even when the chemical composition of the system is preserved, and only the atomic coordinates are varied. This makes the optimization of local basis sets a formidable task. To optimize the basis the configuration which demands the largest (the most complicated, when considering the symmetry) basis must first be found. Then, the same basis must be applied throughout the calculation to maintain the same accuracy and produce comparable results.
In this work, optimization is performed by testing the basis in a slab calculation, where the oxygen molecule lies sufficiently far from the surface that there is negligible interaction. The extent of the basis is optimized to minimize the energy of a system, where the slab-molecule distance is 3.0 Å. At this distance the wavefunctions is so small that the contribution of the basis functions to the total energy is easy to approximate. Furthermore, the shape of the basis for the oxygen is optimized when positioned 1.35 Å from the surface, where the polarization of the molecule is at its maximum. Adding d-symmetry basis functions to the oxygen yields much better results than a basis comprising only p and s symmetries. The main aim of the testing is to generate basis functions that work well far away from the surface as well as yielding a converged adsorption energy for atomic oxygen. Furthermore, the basis sets for both oxygen and copper are tested by applying them to a Cu-O dimer, which is believed to show the worst behaviour with respect to basis size.
Another question is the transferability of pseudopotentials. Although, the norm-conservation constraint should improve the transferability of pseudopotentials, in many cases this is not sufficient to ensure accurate results. The pseudopotentials as well as the basis functions must be carefully tested with the environment that they will have in the models in which they are going to be applied. For example, Kiejna *et al.* [71] observed that when an atom is placed in an environment where it has a considerably smaller bond length than the one in which the pseudopotential was created for, this can result in a poor description of the system. They modelled CO oxidation on $RuO_2(110)$ surface, using a standard pseudopotential approach, together with full-potential calculations. The two results differ; however, this is not due the frozen core approximation used in the pseudopotential calculations.

Instead, scattering properties of the Ru f-orbitals turn out to be responsible for the discrepancy.

Chapter 4

Review of the Calculations

Publications related to this work cover the oxidation problem from a clean Cu(100) surface to the oxygen precovered surface, and finally, the oxygen induced reconstruction. For clean Cu{100} surfaces the effect of point defects e.g. vacancies, as well as substitutional Ag atoms, on the adsorption of O_2 are studied. In two of the papers, a more realistic experimental situation is investigated by taking into account the effect of monoatomic steps. The guiding line for the calculations has been the idea to resolve the features that are most important for the chemical reactions.
This chapter is structured as follows. First, the reaction on a clean Cu(100) surface is discussed. Next, the discussion proceeds to oxygen precovered surfaces. Finally, the results of the comparison between different materials are shown, together with conclusions.

4.1 Clean Cu(100)

Publication I examines O_2 on a clean Cu(100) surface within the framework of adiabatic PES calculations. This is essentially a re-examination of the previously published work in Ref. [19] involving recalculation of reaction trajectories by using a different method. Furthermore, the adsorption energies for atomic oxygen on the surface are calculated according to the method suggested by Gajdos *et al.* [72]. They suggest that the reference energy for the adsorption energies is taken as half of the energy of an O_2 molecule in its gas phase triplet state,

$$E_{\mathrm{ads}} = E_{\mathrm{slab}+n\mathrm{O}} - E_{\mathrm{slab}} - n\frac{E_{\mathrm{O}_2}}{2}, \tag{4.1}$$

where $E_{\mathrm{slab}+n\mathrm{O}}$ is the total energy of the system including the oxygen adatoms, E_{slab} is the energy of the slab without oxygen, $E_{\mathrm{O}_2}/2$ is the energy of half of an oxygen molecule with $S = 1$, and n is the number of oxygen atoms in the system.
The calculated energies are summarized in Table 4.1.

Site	E_{ads} [eV]
Hollow	2.4
Bridge	1.7
Top	0.6
Substitutional	1.4

Table 4.1: The adsorption energies for an oxygen atom on a Cu(100) surface. The adsorption energy decreases as the coordination of the oxygen atom is lowered. The substitutional site has the same coordination as the hollow site; however, to satisfy the shorter bonding distance of Cu-O, relaxation of Cu atoms towards the oxygen is needed, and this costs the difference in energy.

The calculated energetics show that the oxygen overlayer occupies the fourfold sites on a Cu(100) surface, following the face centred cubic stacking. The hollow site is favoured by more than 1 eV over sites with lower symmetry. For the dissociation process, the earlier results of Alatalo *et al.* [19] are confirmed, i.e. there is no barrier to adsorption in the entrance channel. This indicates a critical discrepancy between the experimental results reported in Ref. [15] and the present *ab initio* calculations with respect to the actual sticking of the molecules. Theory predicts there is a weakly bound molecular chemisorbed state on the surface, where the adsorption energy is 0.8 eV. The dissociation energy for this site is only 0.51 eV, according to the calculations (Publication II).

The existence of this state is already known from experiments, where Yokoyama *et al.* [17] observed that at low surface temperatures $\approx$ 100 K, the lifetime of the molecular state above the hollow site is sufficiently long to be detected. However, the experimental results show a small tilt angle for the molecule, whereas the current theory predicts that it adopts a lateral orientation. This might be the result of a thermal buckling effect. The present results can be justified by the fact that the molecule and the hollow site are both symmetric; therefore, a the reported tilt is not expected to occur.

The lifetime of this state is determined by the Arrhenius law rate equation,

$$k = A \exp\left(-\frac{E_b}{RT}\right), \tag{4.2}$$

where k is the frequency factor [s^{-1}], E_b is the activation energy, R is the gas constant, and T is the temperature. However, it is unsafe to draw firm conclusions on the basis of these calculations, owing to the expected error margin of the approximations used. The prefactor can be estimated to be approximately the surface phonon frequency, $A = 4.3 \times 10^{12}$ Hz [73]. The lifetime of the molecular adsorption state can be interpreted to be the inverse of the frequency factor. The calculation gives lifetimes of 3×10^3 s and 8×10^{-6} s for 140 K and 300 K surface temperature,

Mode	0.1 Å [eV]	0.05 Å [eV]
S1	0.24	0.24
S4	0.31	0.38
S6	0.28	0.31

Table 4.2: The O_2 dissociation barriers for different phonon modes at a fourfold hollow site on a Cu(100) surface at amplitudes 0.05 Å and 0.1 Å, corresponding to 2% and 4% of the bulk Cu bond length.

respectively. Hence, the state is unobservable at room temperature, yet relatively easy to detect at lower temperatures.

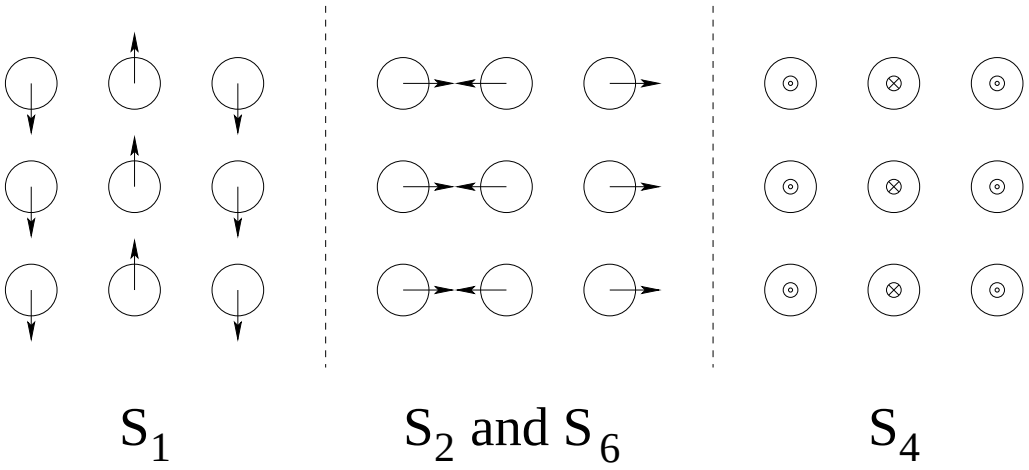

Figure 4.1: Top view of the calculated phonon modes on a Cu(100) surface. S1 is dominated by the collective movement of atom rows in the direction of the row, S2 and S6 are dominated by the collective movement of the atom rows oriented antiparallel to the direction of the rows, and S4 is dominated by the movement of second row atoms, resulting in an alternating pattern of relaxation of the top row atoms.

For O_2 on a perfect Cu(100) surface, the transition state is easy to identify, owing to the fact that the only stable site for the molecule is the four fold hollow site. In molecular dynamics simulations, this will affect the low energy molecules so that they always steer to this particular site, regardless of initial orientation. For defected surfaces this turns out to be much more complicated. In this case PES's contain more than one transition state, and the energy barrier between transition states is difficult to estimate due to the fact that the transition from one minimum to another can proceed via several different routes. For example, the molecule can drag the underlying surface atoms from site to site, and in this manner induce surface atom diffusion. The energetics of such processes, including dynamical movement of the surface atoms, is tedious to find.

In Fig 4.1, a schematic picture of the phonon modes considered on a Cu(100) surface is shown. The modes are described in more detail in Ref. [73]. The calculations show correlation between the phonon amplitudes, phonon modes, and the dissociation barriers for O_2 molecules trapped in hollow sites. The barrier decreases as the amplitude of the phonons increases for the S1 mode. Moreover, the amplitude increases as the temperature is increased. Thus, at 300 K the dissociation barrier is lower than at 140 K, making the lifetime even shorter at higher temperatures than expected from Arrhenius' law. The dissociation barriers with two different amplitudes for each calculated phonon mode are gathered in Table 4.2.

Two dimensional cuts through the six dimensional PES for O_2 on a clean Cu(100) surface are calculated for the trajectories that previous MD calculations suggest they warrant closer investigation. One of these slices is shown in in Fig. 4.2. It represents the PES for an O_2 molecule approaching a hollow site. The shape of the PES is interesting, because it exhibits no barrier for the molecular adsorption, and the shape of the PES also shows indications of a steric hindrance effect [74]. It can be explained, according to the MD simulations, as follows. A molecule traversing the trajectory accelerates towards the surface as it passes through the entrance channel. When it arrives at the minimum, the directions of the forces change discontinuously towards bond elongating and repulsive orientation. At this point the molecule possesses significant momentum directed towards the surface. The small mass of the molecule results in a delay in the change of the direction of motion; hence, the molecule is unable to follow the minimum energy route, and consequently it arrives at the bottom of the PES graph. In this region, the momentum of the molecule towards the surface is already cancelled, and it starts to move upwards. The end result is a slowly decaying oscillation in the direction perpendicular to the surface. Finally, the molecule ends up at the metastable molecular orientation at the minimum of the PES.

This is a good example not only due to its importance for the oxygen adsorption process, but also for the reason that it shows how complicated the interpretation of the reduced dimensional PES figures can be. If the PES exhibits a sharp bend, then the energetics of the molecule-surface interaction is likely to dominate, and the energy transfer from the molecule to the surface will also be efficient. These bends in the PES will cause the molecule not to follow the minimum energy route, but instead take a path that tends to preserve the potential energy in some other form, such as vibrations or rotations. A schematic example of a molecular trajectory with vibrational excitation for the molecule is shown in Fig. 4.3, representing the same molecular orientation as in the previous figure.

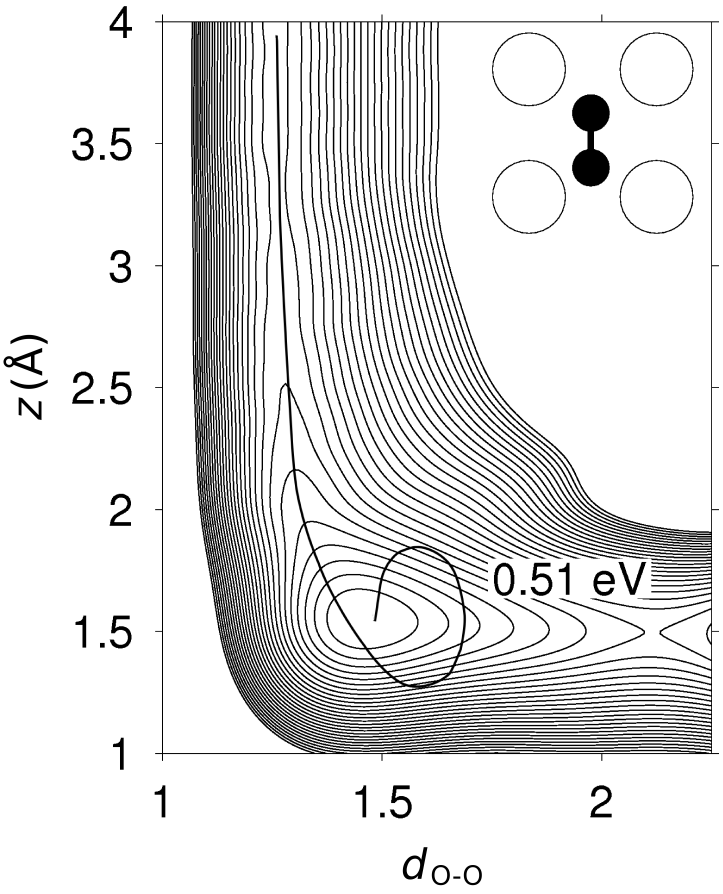

Figure 4.2: Two dimensional slice of the six dimensional PES representing an O_2 molecule approaching a hollow site on Cu(100). The line shows a schematic example of a possible dynamical trajectory for a molecule without initial vibrational excitations.

4.2 Oxygen covered and doped Cu(100)

In Publication I, the effect of on-surface oxygen on the dissociation event is considered. In the calculations on-surface oxygen exhibits a repulsion towards the gas phase oxygen; however, the effect dies out in a relatively short distance. Due to the short screening length the pre-adsorbed oxygen atoms, low coverages are not effective in blocking the incoming molecules. The only method that remains is the physical blocking of the fcc sites, which are also favoured by oxygen molecules.
The sticking of gas phase oxygen on a $2(\sqrt{2} \times \sqrt{2})R45°$O/Cu(100) surface is described in Publication III. The methods applied are novel in the sense that the sticking behaviour of O_2 is investigated by employing static PES calculations in conjunction with *ab initio* molecular dynamics calculations. A criticism of MD is that quantitative results cannot be achieved without employing statistical methods. Nevertheless, it does provide good qualitative understanding of the intensity of the

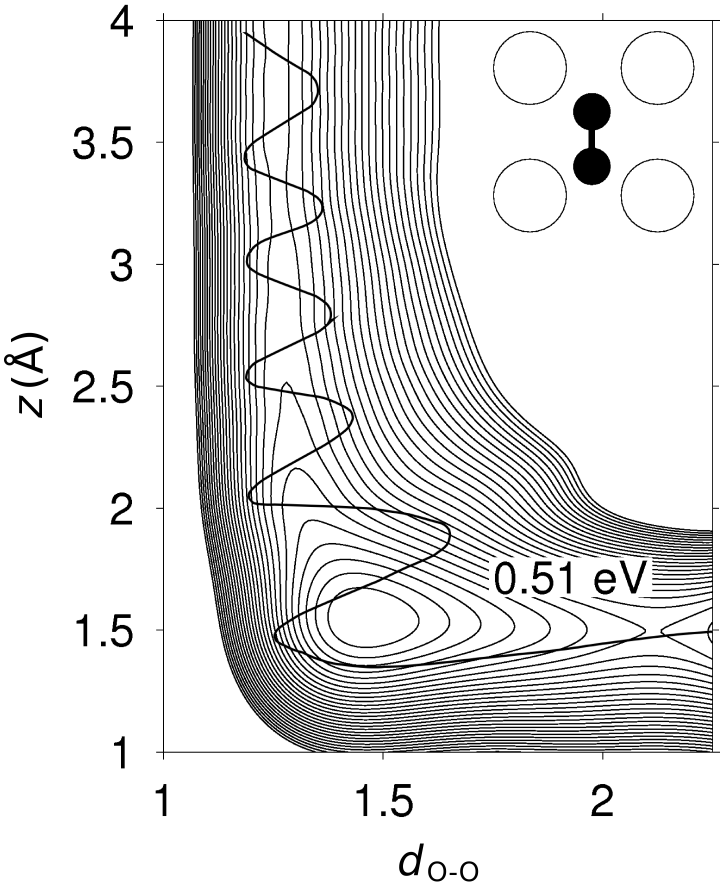

Figure 4.3: The effect of vibrational excitations of the molecule shown on a PES figure. The amplitude of the vibrations increases closer to the surface, and eventually leads to dissociation. The trajectory of the oscillations is schematic.

steering effects, and thereby narrows down the PES trajectories needed to a more manageable number. Using both methods together, it is more feasible to find the minimum energy pathway than by applying the PES method alone.

In Publication III, the adsorption picture for a clean surface is also complemented by studying the effect of pre-adsorbed Ag on Cu(100). This demonstrates that pre-adsorbed Ag makes the Cu(100) surface locally inert towards the adsorption of O_2. In spite of the local reduction in the sticking of O_2, the Ag-doping idea, which is commonly used in the industry, proved to be relatively ineffective. In further computational studies by Kangas *et al.* [75], it is observed that, due to the energetics of Cu-O bonding, Ag atoms at equilibrium diffuse away from the surface forming a layered structure together with Cu. In the structure, a copper-oxide layer is on top, with a Ag-Cu layer immediately below, and the supporting substrate is nearly clean, bulk Cu. Similar results were obtained earlier using experimental X-ray Photoelectron Spectroscopy [76].

To complement the ideas developed in Publication III, the results of a more quantitative investigation into the energetics of O_2 on $2(\sqrt{2} \times \sqrt{2})R45°$ O/Cu(100) are reported in Publication IV. At this point, it was observed experimentally that, after increasing the oxygen concentration, the resulting oxidule phases also exhibit a similar kind of elongated growth behaviour as the reconstructed phase. Hence, it is natural to assume that the oxidule phases grow above the reconstructed phase. The energetics reported in Publication IV demonstrate conclusively that the adsorption of oxygen molecules on the reconstructed phase is never stable. The adsorption energy varies depending on site from -0.1 eV to $+0.8$ eV, indicating only weak attraction or fairly strong repulsion. Moreover, the diffusion barriers are in the range 1.4–2.0 eV making them considerably larger than for a clean Cu(100) surface [19]. The dissociation barriers for the surface are 3.2–4.6 eV; therefore, at ordinary temperatures molecules rarely dissociate.

The energetics directly exclude the possibility of direct adsorption and dissociation of O_2 on the reconstructed phase. Therefore, the mechanism for the migration of oxygen atoms needed for the growth process remains unknown. There are some suggestions that the reconstructed phase boundaries—which, due to their size, cannot be modelled with present resources—are the only sites on the surface that could serve as a starting point in the formation of oxidule islands. Support for this idea comes also from experiments, where oxidule island growth originates at certain discrete points on the surface [77]. Furthermore, strain is likely to be present in the boundary region, and this will reduce the repulsive effect, which the pre-adsorbed oxygen exhibits towards to the gas phase oxygen. Moreover, the phase boundaries suffer large strains due to the mismatch between the missing row reconstructed areas and the second layer. Further indications that such conditions increase the overall reactivity of a clean a Cu(100) surface are found in the present work. For example, the static phonon calculations—which are essentially adsorption calculations for a strained Cu(100)—indicate that only a small strain is needed to lower dissociation barriers. The stress effect is supported experimentally by Uesugi-Saitow *et al.* [78], and predicted to occur for other surfaces [79]. Uesugi-Saitow and co-workers also show that the external strain lowers the dissociative sticking in the case of reconstructed O/Cu(100). Due to the complexity of the surface, this can be interpreted in several ways: it might be that the strain effect is missing entirely for the reconstructed phase, or the applied external stress somehow interferes with the internal stress caused by the reconstruction, and consequently lowers the sticking.

What makes the phase boundaries even more interesting, is that the excess Cu from the reconstructed phase probably diffuses to the boundary areas, due to Cu-O repulsion. The quantity of Cu atoms missing from the reconstructed structure is about 0.5 ML. This is a significant proportion of substrate, which could easily form reactive substrate clusters, or in other ways contribute to oxide growth. In this case, at the boundaries, there are more Cu atoms to react with gas phase O atoms,

thereby increasing the overall reactivity of the boundary regions.
To map the entire six dimensional PES for an O_2 molecule on the reconstructed surface is impractical, owing to the broken symmetry of the surface. Mapping of the full PES including the phonon modes of the surface is impossible. To avoid this, a combination of *ab initio* MD and PES calculations are applied. This approach is particularly useful in the corrugated potential of the reconstructed phase. The MD calculations provide an indication of the stability of the PES trajectories, and test whether the calculated trajectories are local minima or saddle trajectories in energy, thus adding confidence to the limited number of PES trajectories.

4.3 Structurally modified Cu(100)

Structural modifications investigated in this work include vacancies, divacancies, added Cu atom and dimer, stepped (510) (Publication II), and a (211) stepped surface (Publication V). For the adatoms it is found that, contrary to what might be anticipated, the lower coordination of a Cu atom sitting on a hollow site, does not increase the overall reactivity. In fact, the added atoms are chemically more inert to dissociation of O_2 than on a smooth Cu(100) surface. Comparing this result to the case of vacancies and divacancies, where the overall reactivity is increased by lower coordination, suggest that in the first case the oxygen molecule is bonding to the adatom; thus, both of the oxygen atoms in the molecule are bound to the same atom. In this case there is no net force pulling the atoms apart, which results in a higher barrier to dissociation. In the case of a vacancy, however, the unsaturated bonds are distributed around the Cu atoms surrounding the vacancy. In this case—since the oxygen molecule is trying to saturate its bonds—the Cu atoms are drawing the oxygen atoms apart; therefore, the net force for the oxygen atoms is towards the Cu atoms. This lowers the dissociation barrier (see Fig. 4.4).
First principles MD is also used in this work to investigate the stability of the adsorption trajectory over the vacancy site. It is found that the trajectory over the vacancy site is at least metastable, given that the molecules approaching the vacancy with parallel alignment end up in the dissociated state with their oxygen atoms attached to opposite sides of the vacancy. However, the molecules starting from other positions do not end up in the vacancy, nor do the molecules approaching the vacancy directly go to any other site than the vacancy. Naturally, the statistics of these calculations are poor; however, these results do at least indicate that there is no strong steering mechanism pushing molecules away from the vacancy.
An interesting phenomenon has been seen once in the MD simulations at a hollow site next to a vacancy. An oxygen molecule in a chemisorbed state pulled one of the next nearest Cu atoms to the vacancy, moving the vacancy away from the molecule (see Fig 4.5). This is a direct indication, firstly, of the mobility of the surface atoms on the Cu(100); and secondly, of the strength of the bonding between O_2

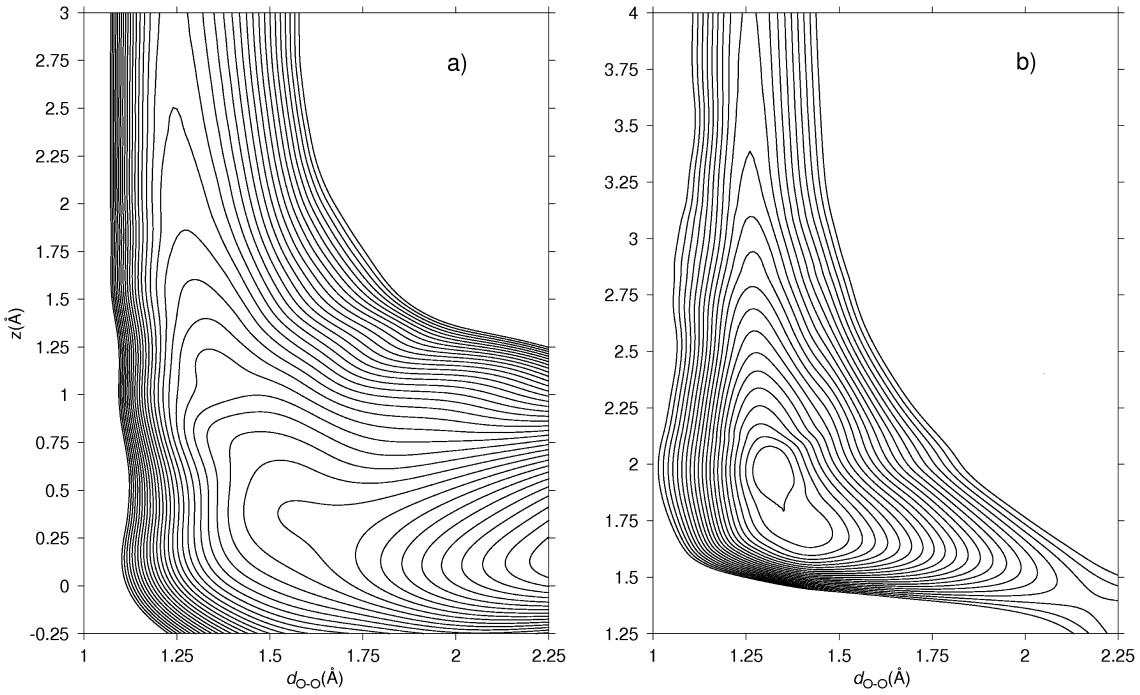

Figure 4.4: The 2-dimensional PES for an O_2 molecule approaching a) a vacancy b) a Cu adatom. Note the missing late barrier in a) compared with the barrier in b).

molecule and surface atoms. While considering the final state of the configuration it has to be noticed that this must be the lowest energy state for adsorbed molecular oxygen. At the final configuration all the energetically favourable O-Cu bonds are saturated. Experimental evidence of adsorbate induced vacancy diffusion is not available, probably due to the fact that the process occurs in timescales of a few hundred femtoseconds. However, adsorbate mediated vacancy diffusion processes have been observed with O_2 on TiO_2 [80] suggesting that the interaction between the adsorbate molecules and the substrate can be intense.

Publication V compares O_2 adsorption pathways on the {211} surfaces of Pd and Cu. These two materials make a good choice since their electronic structures are closely related ($4d^{10}\,5s^0$ and $3d^{10}\,4s^1$ for Pd and Cu, respectively). The property that distinguishes them with regard to structure is the lattice parameter (experimental values of 3.61 Å for Cu and 3.89 Å for Pd [70]). The calculations show that on both materials O_2 molecules favour the hollow sites on the (100) microfacet. This is inevitable since they are the only four fold sites on the surfaces. The relative reactivity of the materials, can be explained by the difference in their lattice parameters. The dissociation barrier for O_2 on a four fold site is larger on Cu than Pd (Fig 4.6). When an oxygen atom passes through a bridge site during the dissociation process—which is considered to be the transition state between the molecular and the adsorbed state—the O-O distance is smaller on Cu than Pd due to the difference

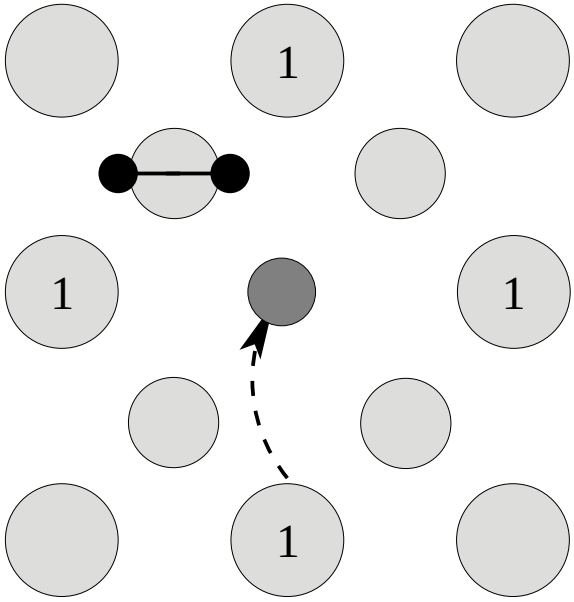

Figure 4.5: A schematic diagram showing how oxygen induced vacancy diffusion occurs on a Cu(100) surface. The intense bonding between the oxygen molecule and the surface Cu atoms attracts the next nearest Cu atom to the vacancy inducing vacancy diffusion away from the adsorbed O_2 molecule. The surface atoms labelled 1 are the ones closest to the vacancy.

in the lattice parameter; hence, the O-O distance is less, and the binding between the O atoms is stronger.

Overall, a Cu(211) surface exhibits a significantly greater reactivity than a clean Cu(100) surface. For O_2 dissociation, a (100) microfacet has similar characteristics to a Cu(100) surface, except that the late barrier is considerably lower for the microfacet. This is explained by the smaller coordination number, together with a suitable geometrical configuration. The lower coordination not only affects the barrier, but also makes the stepped surface more attractive towards oxygen compared with a Cu(100) surface. When comparing the results with a Cu(510) surface (Publication II) it is noteworthy that the adsorption energies are considerably higher on a Cu(211) surface. The differences in the energies are due to the fact that, even though {510} surfaces have terraces with {100} facets and {211} surfaces have terraces with {111} facets, suggesting that Cu{211} surfaces should be less reactive, the microfacets are oriented in [100] directions, and the step density is higher on Cu{211} surfaces. Moreover, {100} microfacets on {211} have undercoordinated atoms at their edges making them more attractive than microfacets on {510}.

The calculated results for the Cu(510) surface can also be compared with the experimental data by Vattuone *et al.* [81]. They observed that the presence of steps on a Cu(410) surface exposed to O_2 with low incident energies makes surface more reactive, while at higher energies the effect is not seen. In agreement with this, the

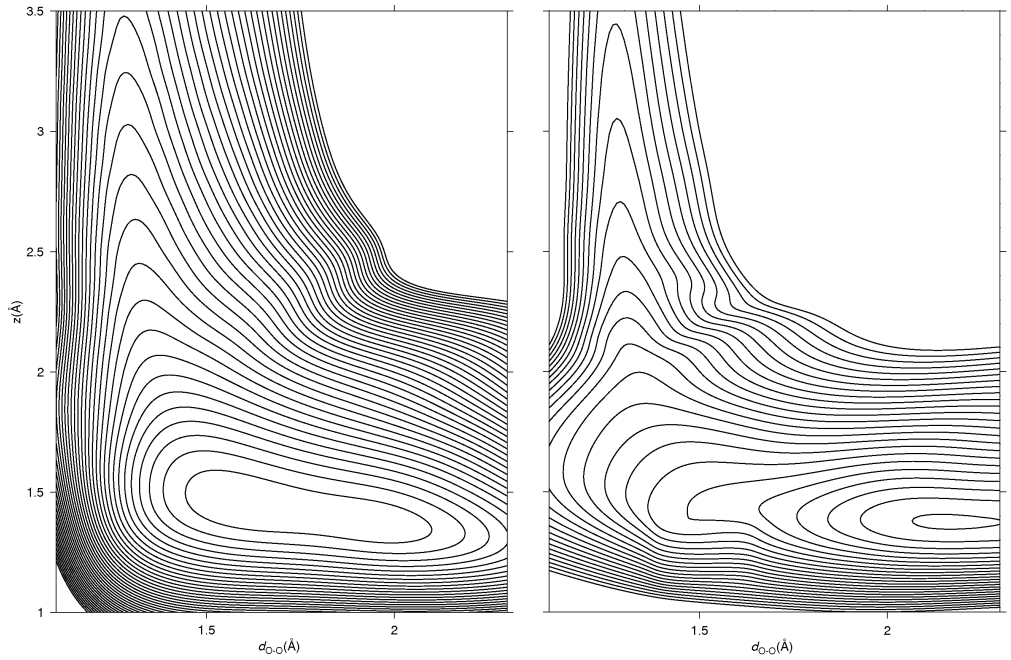

Figure 4.6: The 2-dimensional PES for O_2 on the hollow site of the (100) microfacet on a) Pd, b) a Cu stepped (211) surface. There is no barrier in either case, but the downhill is larger for Pd.

models a Cu(510) surface in this work show that dissociation which occurs at step edges possess with a lower barrier than on a terrace. However, matters are complicated by the fact that terrace hollow sites in the model are more attractive than the most reactive sites at step edges (see Fig. 4.7). For molecules arriving at hollow sites on terraces, this means they must first move to step edges before dissociation can occur with the lower barrier: the step edges increase the reactivity only for molecules arriving directly on the step. The molecules arriving on terraces, will experience the same reactivity as the ones on a clean Cu(100) surface. Here the difference between {510} and {410} planes must also be considered: {410} planes have terraces that are narrower by one atomic row than those of {510}. In practise this means that sites having the same properties as the most attractive ones on {510} surfaces do not exist on {410}. This means that the step edge reactivity is even more apparent on {410}.

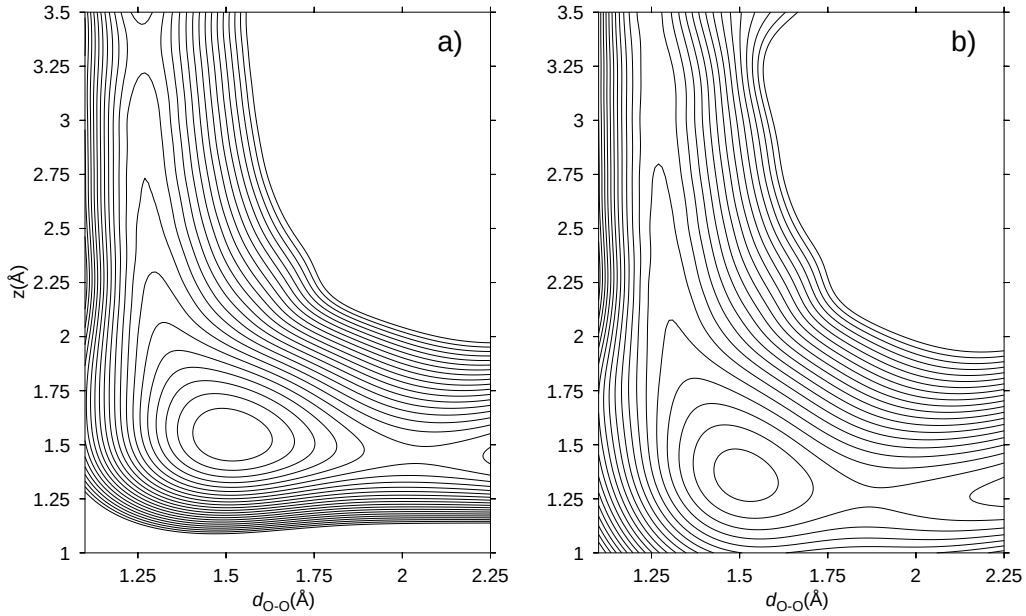

Figure 4.7: The 2-dimensional cuts of the PES for an O_2 molecule on the hollow site of a) {100} terraces, and b) {110} microfacets on Cu{510}. Sites b) have the lowest dissociation energy, and sites a) have the largest adsorption energy.

Chapter 5

Concluding Remarks

When performing calculations to interpret experimental results there are several crucial points to consider. First, it is important to ensure that the experiments and the calculations are performed for the same system. This seems simple, yet when considering the details, real materials posses defects such as thermal vacancies, contaminants, and grain boundaries that may be missing from a model of it. Whether the defects are important depends on the particular system. Another important matter to consider is the fact that the timescales and sizes in experiments are microscopic (μs, nm), while *ab initio* theory involves timescales and sizes at the picoscale (fs, Å). Neglecting this can lead to serious misinterpretations. A multiscale modelling approach is likely to be needed to go from the *ab initio* length and timescales to the experimental ones. Furthermore, the correctness of the theoretical model must be ensured. There are several systems where it is known that the current approximations fail. For example, as mentioned in Chapter 3, DFT-based methods perform poorly for systems with strong correlation effects. Although the lattice structures are usually satisfactory, the electronic states might not be described properly. Furthermore, DFT is a groundstate theory. The electronic states do not correspond directly to the real ones, but are instead quasiparticle states in the form of a mathematical representation of the groundstate. States above the Fermi level are usually wrong due to the fact that when an electronic excitation occurs, the states below the Fermi level must also change owing to electron-electron correlation effects [64].

The main results of this thesis show that there are several structural properties determining the reactivity of a metal surface. Oxygen molecules are affected critically by the underlying atomic configuration, and always aim to achieve four fold symmetry. When this symmetry is broken, the adsorption energy is lowered; however, this may also lower barriers to dissociation. This effect is demonstrated by the "frozen phonon" calculations reported here, where the character of specific phonon modes even at low displacements makes activation energies small via low symmetry configurations (see Fig. 5.1). In the calculations, where an O_2 molecule dissociates without

a barrier over a vacancy site, both atoms in the molecule try to reach the equilibrium bonding distance between the surface atoms. In forming Cu-O bonds, the O-O bond of the O_2 molecule is opened, allowing it to dissociate. This is determined by the geometry of the site. Thus, the lowering of the barrier can be estimated by subtracting the energy of an O-O bond from four times the energy of a Cu-O bond.

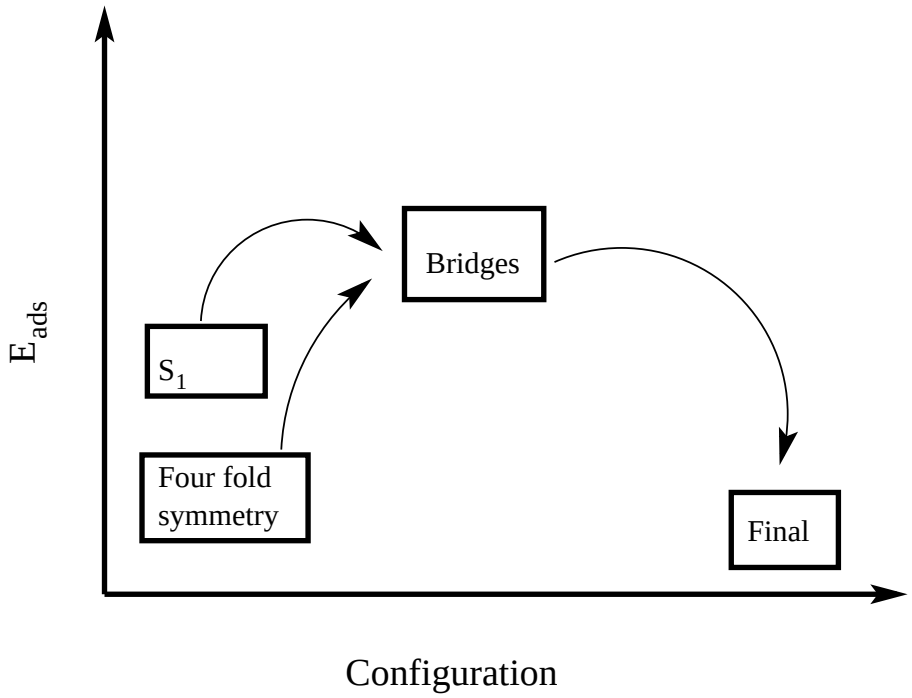

Figure 5.1: Lowering the symmetry causes the reference state to be unfavourable.

The investigation into reconstructed oxygen precovered Cu{100} surfaces reported in publications III and IV eliminates one suggested mechanism for oxide formation. Although the result appears unremarkable on its own, it has important consequences for the overall process. Following reconstruction, most of the surface no longer actively participates in the oxide formation process at low temperatures. Note that the boundaries of the reconstructed areas are not included in the models.

In the course of the present work, the frozen surface approximation—a standard tool in surface science—is re-evaluated. The weakness of this approximation is that important degrees of freedom are neglected. A means to circumvent the problem is proposed. First, *ab initio* Molecular Dynamics are employed to provide an improved description of the energy dissipation pathways during surface-adsorbate interactions. Then, it is proposed that this qualitative description can be improved upon by allowing surface atoms that are involved in heat dissipation to move, instead of being fixed. This method is justified on the basis of molecular dynamics simulations, which show that there is only small movement (apart from the thermal fluctuations) of the atoms next nearest to the reactants. Thus, it can be assumed that the next

nearest atoms do not contribute as much in the heat dissipation during the reaction as the main participants in the reaction. This reduces the computational burden by orders of magnitude, due to the reduced degrees of freedom, and allows new insights into the reaction dynamics.

Future work. This work demonstrates the feasibility of calculating sticking coefficients and means by which it may be achieved with a satisfactory level of accuracy at the *ab initio* level of theory. However, there are several drawbacks that must be considered. For example, the models described in Ref. [22] are based on the frozen substrate approximation, which assumes there is no transfer of heat between the substrate and the adsorbents. The present work shows clearly that heat transfer is not negligible, and when disregarded may lead to incorrect conclusions. Thus, the method is suitable only for systems where the early barrier at the entrance channel dominates. For systems which have barriers closer to the surface, the problem of strong heat transfer, and even coupling between the dissociation events and surface phonons must be addressed.

A fully dynamical model in conjunction with statistical methods would be the ideal way to achieve this; however, present computer resources are far from sufficient. Nevertheless, remedies for this situation are now available. Careful testing conducted during the course of this work reveals that the computational burden can be reduced by an order of magnitude by optimizing finite basis sets, and keeping the basis as small as possible. For example, basis functions associated with atoms that are not chemically active during the adsorption process, and can be considered as bulk atoms, can be treated more approximately than is necessary for those in more critical situations. Recently, a hybrid filtering method [82] has been developed which permits smaller mesh cut-offs to be used without increasing the "egg-box effect", which is currently a problem with all methods involving integration in real space. Normally, changes in atomic coordinates relative to the supercell when the density of the integration mesh is not sufficient, artificially affect to the total energy. These improvements mean that in the near future it may be possible to apply *ab initio* MD with statistical methods, and even obtain quantitative information concerning the transfer of heat during the initial deposition.

Universality of the results. The current results mainly consider the oxidation of Cu{100} surfaces. However, several conclusions drawn here are expected to be valid for other metals. For example, the dissociation of O_2 via a four fold site is also observed on a Pd(100) surface (Publication VIII). For Pd(100) the dissociation mechanism is similar to that on Cu(100); however, the reaction barriers are different. The reconstruction occurs also on O/Ag(100) so the results for the reconstructed surface can be expected to be appropriate for Ag{100} surfaces as well. These trends can be applied to other metals; however, the energetics must be recalculated for different substrates.

Bibliography

[1] M. Boncheva, D. A. Bruzewicz, and G. M. Whitesides, "Millimeter-scale self-assembly and its applications," *Appl. Chem.*, vol. 75, p. 621, 2003.

[2] D. Gracias, J. Tien, T. L. Breen, C. Hsu, and G. M. Whitesides, "Forming electrical networks in three dimensions by self-assembly," *Science*, vol. 289, p. 1170, 2000.

[3] H. O. Jacobs, A. R. Tao, A.Schwartz, D. H. Gracias, and G. M. Whitesides, "Fabrication of a functional cylindrical display using solder-based self-assembly," *Science*, vol. 296, p. 323, 2002.

[4] A. Groß, *Theoretical Surface Science A Microscopic Perspective.* Berlin: Springer, 2003.

[5] J. Liu, M. Xu, and F. Zaera, "Determination of the rate limiting step in the oxidation of CO on Pt(111) surfaces," *Catal. Lett.*, vol. 37, p. 9, 1995.

[6] D. J. Burnett, A. T. Capitano, A. M. Gabelnick, A. L. Marsh, D. A. Fischer, and J. L. Gland, "In-situ soft x-ray studies of CO oxidation on the Pt(111) surface," *Surf. Sci*, vol. 564, p. 29, 2005.

[7] H. Over and A. P. Seitsonen, "Oxidation of metal surfaces," *Science*, vol. 297, p. 2003, 2002.

[8] G.-C. Wang, L. Jiang, X.-Y. Pang, Z.-S. Cai, Y.-M. Pan, X.-Z. Zhao, Y. Morikawa, and J. Nakamura, "A theoretical study of surface-structural sensitivity of the reverse water-gas shift reaction over Cu(hkl) surfaces," *Surf. Sci*, vol. 543, p. 118, 2003.

[9] L. Jiang, G.-C. Wang, Z.-S. Cai, Y.-M. Pan, and X.-Z. Zhao, "Promotion of the water-gas shift reaction by pre-adsorbed oxygen on Cu(hkl) surfaces: a theoretical study," *J. Mol. Struct.*, vol. 710, p. 97, 2004.

[10] T. Sueyoshi, T. Sasaki, and Y. Iwasawa, "Oxygen atoms on Cu(100) formed at 100 K, active for CO oxidation and water-hydrogen abstraction characterized by HREELS and TPD," *J. Phys. Chem. B*, vol. 101, p. 4648, 1997.

[11] N. Cabrera and N. F. Mott, "Theory of the oxidation of metals," *Rep. Prog. Phys.*, vol. 12, p. 163, 1948.

[12] K. Lawless and D. Mitchell, "The low pressure oxidation of copper single crystals," *Mem. Sci. Rev. Metallurg*, vol. 62, p. 17, 1965.

[13] B. Hammer and J. K. Nørskov, "Why gold is the noblest of all the metals," *Nature*, vol. 376, p. 238, 2002.

[14] P. Marcus and J. Oudar, *Corrosion mechanisms in theory and practice*. New York: Marcel Decker, 1995.

[15] P. Junell, M. Ahonen, M. Hirsimäki, and M. Valden, "Influence of surface modification on the adsorption dynamics of O_2 on Cu(100)," *Surf. Rev. Lett.*, vol. 11, p. 1, 2004.

[16] M. Wuttig, R. Franchy, and H. Ibach, "Oxygen on Cu(100)–a case of an adsorbate induced reconstruction," *Surf. Sci*, vol. 213, p. 103, 1989.

[17] T. Yokoyama, D. Arvanitis, T. Lederer, M. Tischer, L. Tröger, , and K. Baberschke, "Adsorption of oxygen on Cu(100). ii. molecular adsorption and dissociation by means of O K-edge x-ray-absorption fine structure," *Phys. Rev. B*, vol. 48, p. 15405, 1993.

[18] I. Langmuir, "The evaporation, condesation and reflection of molecules and the mechanism of adsorption," *Phys. Rev.*, vol. 8, p. 149, 1916.

[19] M. Alatalo, S. Jaatinen, P. Salo, and K. Laasonen, "Oxygen adsorption on Cu(100): First principles pseudopotential calculations," *Phys. Rev. B*, vol. 14, p. 327, 2004.

[20] L. Osterlund, I. Zorić, and B. Kasemo, "Dissociative sticking of O_2 on Al(111)," *Phys. Rev. B*, vol. 55, p. 15452, 1997.

[21] J. Behler, B. Delley, S. Lorenz, K. Reuter, and M. Scheffler, "Dissociation of O_2 at Al(111): The role of spin selection rules," *Phys. Rev. Lett.*, vol. 94, p. 036104, 2005.

[22] J. Behler, *Dissociation of Oxygen Molecules on the Al(111) Surface*. Berlin: TU, 2004.

[23] M. Binetti, O. W. e, E. Hasselbrink, G. Katz, R. Kosloff, and Y. Zeiri, "The role of nonadiabatic pahtways and molecular rotations in the oxygen abstraction reaction on the Al(111) surface," *Chem. Phys. Lett.*, vol. 373, p. 366, 2003.

[24] A. N. Salanov, V. N. Bibin, and V. T. Yakushko, "Structural transformations in overlayer and sticking probability during chemisorption: oxygen on (100) surface of metals," *J. Mol. Cat. A*, vol. 158, p. 367, 2000.

[25] M. Kittel, M. Polcik, R. Terborg, J.-T. Hoeft, P. Baumgärtel, A. M. Bradshaw, R. Toomes, J.-H. Kang, D. P. Woodruff, M. Pascal, C. Lamont, and E. Rotenberg, "The structure of oxygen on Cu(100) at low and high coverages," *Surf. Sci*, vol. 470, p. 311, 2001.

[26] M. Basham, P. A. Mulheran, and F. Montalenti, "Diffusion and stability of small vacancy clusters on Cu(100) – a simulation study," *Surf. Sci*, vol. 565, p. 289, 2004.

[27] R. van Gastel, E. Somfai, S. B. van Albada, W. van Saarloos, and J. W. M. Frenken, "Vacancy diffusion in the Cu(001) surface I: an stm study," *Surf. Sci*, vol. 521, p. 10, 2002.

[28] S. Jaatinen, M. Rusanen, and P. Salo, "A multi-scale monte carlo study of oxide structures on the Cu(100) surface," *Surf. Sci*, vol. 73, p. 1813, 2007.

[29] N. Perron, N. Pineau, E. Arquis, J. C. Rayez, and A. Salin, "Adsorption of atomic oxygen on the Cu(100) surface," *Surf. Sci*, vol. 599, p. 160, 2005.

[30] H. Brune, J. Wintterlin, R. J. Behm, and G. Ertl, "Surface migration of hot adatoms in the course of dissociative chemisorption of oxygen on Al(111)," *Phys. Rev. Lett.*, vol. 68, p. 624, 1992.

[31] S. Y. Liem, J. H. R. Clarke, and G. Kresse, "First principles calculation of oxygen adsorption and reconstruction of Cu(110) surface," *Surf. Sci*, vol. 415, p. 194, 1998.

[32] J. Buisset, H.-P. Rust, E. K. Schweizer, L. Cramer, and A. M. Bradshaw, "Identification of active oxygen on Cu{110} using low temperature scanning tunnelling microscopy," *Surf. Sci*, vol. 349, p. L147, 1996.

[33] H. Dürr, T. Fauster, and R. Schneider, "Surface structure determination of the (2×1) O-Cu(110) reconstruction by low-energy ion scattering," *Surf. Sci*, vol. 244, p. 237, 1991.

[34] F. Jensen, F. Besenbacher, E. Lægsgaard, and I. Stensgaard, "Surface reconstructio of Cu(110) induced by oxygen chemisorption," *Phys. Rev. B*, vol. 41, p. 10233, 1990.

[35] I. K. Robinson, E. Vlieg, and S. Ferrer, "Oxygen-induced missing row reconstruction of Cu(001) and Cu(001) vicinal surfaces," *Phys. Rev. B*, vol. 42, p. 6954, 1990.

[36] M. Lampimäki, K. Lahtonen, M. Hirsimäki, and M. Valden, "Nanoscale oxidation of Cu(100): Oxide morphology and surface reactivity," *J. Chem. Phys.*, vol. 126, p. 034743, 2007.

[37] M. Rocca, L. Savio, L. Vattuone, U. Burghaus, V. Palomba, N. Novelli, F. B. de Mongeot, U. Valbusa, R. Gunnella, G. Comelli, A. Baraldi, S. Lizzit, and G. Paolucci, "Phase transition of dissociatively adsorbed oxygen on Ag(001)," *Phys. Rev. B*, vol. 61, p. 213, 2000.

[38] N. Bonini, A. Kokalj, A. D. Corso, S. de Gironcoli, and S. Baroni, "Structure and dynamics of the missing-row reconstruction on O/Cu(100) and O/Ag(100)," *Surf. Sci*, vol. 600, p. 5074, 2006.

[39] S. Stolbov, A. Kara, and T. S. Rahman, "Electronic structure of the $c(2 \times 2)$ O/Cu(001) system," *Phys. Rev. B*, vol. 66, p. 245405, 2002.

[40] S. Stolbov and T. S. Rahman, "Role of long range interaction in oxygen superstructure formation on Cu(001) and Ni(001)," *Phys. Rev. Lett.*, vol. 89, p. 116101, 2003.

[41] F. Jensen, F. Besenbacher, E. Lægsgaard, and I. Stensgaard, "Dynamics of oxygen-induced reconstruction of Cu(100) studied by scanning tunneling microscopy," *Phys. Rev. B*, vol. 42, p. 9206, 1990.

[42] M. J. Harrison, D. P. Wooddruff, and J. Robinson, "Adsorbate induced surface reconstruction and surface-stress changes in Cu(100)/O: Experiment and theory," *Phys. Rev. B*, vol. 74, p. 165402, 2006.

[43] J. C. Yang, M. Yeadon, B. Kolasa, and J. M. Gibson, "Oxygen surface diffusion in three-dimensional Cu_2O growth on Cu(100) thin films," *Appl. Phys. Lett.*, vol. 70, p. 3522, 1997.

[44] G. Zhou and J. C. Yang, "Formation of quasi-one-dimensional Cu_2O structures by in situ oxidation of Cu(100)," *Phys. Rev. Lett.*, vol. 89, p. 106101, 2002.

[45] J. M. Soler, E. Artacho, J. D. Gale, A. García, J. Junquera, P. Ordejón, and D. Sánchez-Portal, "The SIESTA method for ab initio order-N materials simulation," *J. Phys. Condens. Matter*, vol. 14, p. 2745, 2002.

[46] D. Sánchez-Portal, P. Ordejón, E. Artacho, and J. M. Soler, "Density-functional method for very large systems with LCAO basis sets," *Int. J. Quantum Chem.*, vol. 65, p. 453, 1997.

[47] E. Artacho, D. Sánchez-Portal, P. Ordejón, A. García, and J. M. Soler, "Linear-scaling ab-initio calculations for large and complex systems," *Phys. Stat. Sol. b*, vol. 215, p. 809, 1999.

[48] J. Junquera, O. Paz, D. Sánchez-Portal, and E. Artacho, "Numerical atomic orbitals for linear-scaling calculations," *Phys. Rev. B*, vol. 64, p. 235111, 2001.

[49] E. Anglada, J. M. Soler, J. Junquera, and E. Artacho, "Systematic generation of finite-range atomic basis sets for linear-scaling calculations," *Phys. Rev. B*, vol. 66, p. 205101, 2002.

[50] G. Kresse and J. Hafner, "Norm-conserving and ultrasoft pseudopotentials for first-row and transition elements," *J. Phys. Condens. Matter*, vol. 6, p. 8245, 1994.

[51] G. Kresse and J. Furthmüller, "Efficiency of ab-initio total energy calculations for metals and semiconductors using a plane-wave basis set," *Comput. Mat. Sci*, vol. 6, p. 15, 1996.

[52] G. Kresse and J. Furthmüller, "Efficient iterative schemes for *ab initio* total-energy calculations using a plane-wave basis set," *Phys. Rev. B*, vol. 54, p. 11169, 1996.

[53] G. Kresse and D. Joubert, "From ultrasoft pseudopotentials to the projector augmented-wave method," *Phys. Rev. B*, vol. 59, p. 1758, 1999.

[54] P. E. Blöchl, "Projector augmented-wave method," *Phys. Rev. B*, vol. 50, p. 17953, 1994.

[55] H. J. Monkhorst and J. D. Pack, "Special points for Brillouin-zone integrations," *Phys. Rev. B*, vol. 13, p. 5192, 1977.

[56] A. H. MacDonald, "Comment on special points for Brillouin-zone integrations," *Phys. Rev. B*, vol. 18, p. 5897, 1978.

[57] P. Hohenberg and W. Kohn, "Inhomogenous electron gas," *Phys. Rev.*, vol. 136, p. B864, 1964.

[58] W. Kohn and L. Sham, "Self-consistent equations including exchange and correlation effects," *Phys. Rev.*, vol. 140, p. A1133, 1965.

[59] J. Grotendorst, S. Blügel, and D. M. (Eds.), *Computational nanoscience: Do it Yourself!*, vol. 31. Jülich: John von Neumann institute for computing NIC Series, 2006.

[60] D. Ceperley and B. J. Alder, "Ground state of the electron gas by a stochastic method," *Phys. Rev. Lett.*, vol. 45, p. 566, 1980.

[61] J. P. Perdew, K. Burke, and M. Ernzerhof, "Generalized gradient approximation made simple," *Phys. Rev. Lett.*, vol. 88, p. 3865, 1996.

[62] J. P. Perdew, K. Burke, and Y. Wang, "Atoms, molecules, solids, and surfaces: Applications of the generalized gradient approximation for exchange and correlation," *Phys. Rev. B*, vol. 46, p. 6671, 1992.

[63] C. Filippi, C. J. Umrigar, and X. Gonze, "Separation of the exchange-correlation potential into exchange plus correlation: An optimized effective potential approach," *Phys. Rev. A*, vol. 54, p. 4810, 1996.

[64] R. M. Martin, *Electronic Structure – Basic Theory and Practical Methods*. Cambridge: Cambridge university press, 2004.

[65] M. A. L. Marques, A. Castro, G. F. Bertsch, and A. Rubio, "OCTOPUS: a first-principles tool for excited electron–ion dynamics," *Comput. Phys. Commun.*, vol. 151, p. 60, 2003.

[66] M. Marques and E. Gross, "Time-dependent density functional theory," *Annu. Rev. Phys. Chem.*, vol. 55, p. 427, 2004.

[67] OCTOPUS *manual*, 2007.

[68] M. Born and J. R. Oppenheimer, "Zur quantentheorie der molekaln," *Ann. Physik.*, vol. 84, p. 457, 1927.

[69] N. Troullier and J. L. Martins, "Efficient pseudopotentials for plane-wave calculations," *Phys. Rev. B*, vol. 43, p. 1993, 1991.

[70] N. W. Ashcroft and N. D. Mermin, *Solid State physics*. New York: Brooks Cole, 1976.

[71] A. Kiejna, G. Kresse, J. Rogal, A. D. Sarkar, K. Reuter, and M. Scheffler, "Comparison of the full-potential and frozen-core approximation approaches to density-functional calculations of surfaces," *Phys. Rev. B*, vol. 73, p. 035404, 2006.

[72] M. Gajdoš, A. Eichler, and J. Hafner, "Ab initio density functional study of o on the Ag(001) surface," *Surf. Sci*, vol. 531, p. 272, 2003.

[73] Y. Chen, S. Y. Tong, J.-S. Kim, L. L. Kesmodel, T. Rodach, K. P. Bohnen, and K. M. Ho, "Characterization of surface phonons on Cu(001) and Ag(001): First-principles phonon calculations with experimental and theoretical studies of high-resolution electron-energy-loss spectra," *Phys. Rev. B*, vol. 44, p. 11394, 1991.

[74] A. Groß, S. Wilke, and M. Scheffler, "Six-dimensional quantum dynamics of adsorption and desorption of H_2 at Pd(100): steering and steric effects," *Phys. Rev. Lett.*, vol. 75, p. 2718, 1995.

[75] T. Kangas, N. Nivalainen, H. Pitkänen, A. Puisto, M. Alatalo, and K. Laasonen, "Oxygen induced segregation of copper in to Ag/Cu(100) surface," *Surf. Sci*, vol. 600, p. 6103, 2006.

[76] M. Hirsimäki, M. Lampimäki, K. Lahtonen, I. Chorkendorff, and M. Valden, "Investigation of the role of oxygen induced segregation of Cu during Cu_2O formation on Cu{100}, Ag/Cu{100} and Cu(Ag) alloy," *Surf. Sci*, vol. 583, p. 157, 2005.

[77] M. Lampimäki, K. Lahtonen, M. Hirsimäki, and M. Valden, "Nanoscale oxidation of Cu(100): Oxide morphology and surface reactivity," *J. Chem. Phys.*, vol. 126, p. 034703, 2007.

[78] Y. Uesugi-Saitow and M. Yata, "Influence of external stress on surface reaction dynamics," *Phys. Rev. Lett.*, vol. 88, p. 256104, 2002.

[79] M. Mavrikakis, B. Hammer, and J. K. Nørskov, "Effect of strain on the reactivity of metal surfaces," *Phys. Rev. Lett.*, vol. 81, p. 2819, 1998.

[80] R. Schaub, E. Wahlström, A. Rennau, E. Lægsgaard, I. Stensgaard, and F. Besenbacher, "Oxygen-mediated diffusion of oxygen vacancies on the $TiO_2(110)$," *Science*, vol. 299, p. 377, 2003.

[81] L. Vattuone, L. Savio, M. Okada, K. Moritani, and M. Rocca, "Initial sticking probability of O_2 on Cu(410)," *Unpublished*.

[82] E. Anglada and J. M. Soler, "Filtering a distribution simultaneously in real and Fourier space," *Phys. Rev. B*, vol. 73, p. 115122, 2006.